


1964

Analysis of some biological systems using state variable theory

Duane Ellison Sander
Iowa State University

Follow this and additional works at: <https://lib.dr.iastate.edu/rtd>

 Part of the [Animal Sciences Commons](#), [Electrical and Computer Engineering Commons](#), [Physiology Commons](#), and the [Veterinary Physiology Commons](#)

Recommended Citation

Sander, Duane Ellison, "Analysis of some biological systems using state variable theory " (1964). *Retrospective Theses and Dissertations*. 3883.
<https://lib.dr.iastate.edu/rtd/3883>

This Dissertation is brought to you for free and open access by the Iowa State University Capstones, Theses and Dissertations at Iowa State University Digital Repository. It has been accepted for inclusion in Retrospective Theses and Dissertations by an authorized administrator of Iowa State University Digital Repository. For more information, please contact digirep@iastate.edu.

This dissertation has been 65-4639
microfilmed exactly as received

SANDER, Duane Ellison, 1938-
ANALYSIS OF SOME BIOLOGICAL
SYSTEMS USING STATE VARIABLE
THEORY.

Iowa State University of Science and
Technology, Ph.D., 1964
Engineering, electrical
Physiology

University Microfilms, Inc., Ann Arbor, Michigan

ANALYSIS OF SOME BIOLOGICAL SYSTEMS
USING STATE VARIABLE THEORY

by

Duane Ellison Sander

A Dissertation Submitted to the
Graduate Faculty in Partial Fulfillment of
The Requirements for the Degree of
DOCTOR OF PHILOSOPHY

Major Subject: Electrical Engineering

Approved:

Signature was redacted for privacy.

In Charge of Major Work

Signature was redacted for privacy.

Head of Major Department

Signature was redacted for privacy.

Dean of Graduate College

Iowa State University
Of Science and Technology
Ames, Iowa

1964

TABLE OF CONTENTS		Page
I.	INTRODUCTION	1
II.	STATE VARIABLE THEORY	4
III.	LIAPUNOV'S SECOND METHOD APPLIED TO A NONLINEAR BIOLOGICAL SYSTEM	11
IV.	EXPERIMENTAL VERIFICATION OF PACEMAKER ANALYSIS	29
V.	STATE VARIABLE MODEL FOR CAROTID SINUS HEART RATE REFLEX	38
VI.	EXPERIMENTAL RESULTS FOR CAROTID SINUS HEART RATE REFLEX	52
VII.	THE USE OF STATE VARIABLES TO DESCRIBE A CLOSED LOOP FEEDBACK SYSTEM	68
VIII.	CONCLUSION	74
IX.	LITERATURE CITED	77
X.	ACKNOWLEDGEMENTS	80
XI.	APPENDIX A	81
XII.	APPENDIX B	94
XIII.	APPENDIX C	99

I. INTRODUCTION

In developing a quantitative understanding of physiological reflex arcs and some biological control systems, two characteristics consistently contribute to the difficulty of mathematical formulation and analysis. One problem is the nonlinear elements which are always present and the other is the manner in which signals are transmitted, along neural pathways, from one physiological unit to another. It has been well accepted that the information transfer is accomplished by a distribution of impulses in time, or pulse frequency modulation (18). The difficulties arise, mainly, in formulating the mathematical description of systems of this type, i.e., systems containing both nonlinearities and transmitting information from one functional unit to the other by pulse frequency modulation. This is the problem considered in this thesis and a relatively new control theory method has been used in order to evaluate the advantages and disadvantages in using this method when analyzing a problem of the type just described.

Mathematical descriptions of nonlinear systems usually consist of linearized approximations for the nonlinearities and this technique often limits the range and flexibility of the variables studied (34). The state variable formulation, introduced in the last few years, has become an important tool in the analysis of nonlinear as well as linear control systems. The state variable formulation does not necessarily eliminate all of the difficulties of nonlinear problems, but it does provide a systematic approach for the analysis of such problems.

Since the systems to be studied deal with a form of pulse frequency modulation, it was hoped that some literature would be available on this

subject. A theoretical analysis of pulse frequency modulation was written by Ross (28) in 1949, and he derives limits on certain variables in order to be assured that the pulse frequency is periodic after modulation. This is a rather restricted case in as far as biological systems are concerned. A general treatment of sampled-data systems, of which this topic is a special case, has been discussed by Hufnagel (17). He presents methods for analyzing aperiodically-sampled-data systems. Many of these methods are linearized approximations for the physical system discussed. Work reported in the biological area has been done by Jones, et al. (18) and Rashevsky (27). Although other material has been written, these seem to be the most significant contributions to this field of study. Even though these people have worked on this topic and arrived at different methods of analysis, it seems that there is more to be done both experimentally and theoretically.

Many biological control systems have been analyzed by conventional control system techniques and an excellent literature survey of biocontrol systems analysis has been presented by Jury and Pavlidis (19). It is felt that the pulse frequency information and nonlinearities of these systems can be advantageously incorporated in the state variable formulation of these problems (11). By using this formulation, and the definition of instantaneous pulse frequency by Jones, et al. (18), information can be injected into a control system with no approximations or linearizations associated with it. It is believed that by analyzing a specific system with this technique, helpful conclusions may be drawn as to its usefulness in biological control system research. Therefore, this thesis uses the state variable formulation in an analysis of the control system which

regulates heart rate, and from this analysis an evaluation of the use of the state variable formulation in biological systems is made.

For those not familiar with state variable theory, a short introduction is contained in the second chapter. This treatment will give sufficient background for the analysis of the remainder of the thesis.

The specific problem of controlling heart rate by vagal stimulation of the pacemaker is considered and Liapunov's Second Method used to obtain conditions for stability of the concentration of acetylcholine at the pacemaker site or sinoatrial node. This concentration is related to the period of heart rate and experiments are conducted to substantiate theoretical predictions.

State variable theory is used to simulate the carotid sinus heart rate reflex and experimental results are compared to calculated results. This is done in order to evaluate the injection of pulse frequency information into the state variable simulation.

In order to illustrate the use of state variables in a closed loop system, a model of the carotid sinus heart rate control loop is postulated, and the state variable equations are found. This model is not analyzed due to lack of knowledge of the influences affecting cardiac muscle.

In conclusion, the advantages and disadvantages of the state variable formulation are discussed. Following this discussion, a number of possible extensions of the work are pointed out and explained briefly.

II. STATE VARIABLE THEORY

A. Introduction

Since this report may be of interest not only to those familiar with state variable theory but also to people whose technical experience is not closely connected with control system analysis, an introductory treatment of state variable theory is included. The chapter will deal with the definitions and manipulations necessary to follow the subsequent application of this theory. This will not be a complete treatment of the theory. The interested reader is referred to L. A. Zadeh and C. A. Desoer's (40) book of adapting the formulation to digital computer manipulations is presented.

B. Theory

The key observation which explains the use and mechanics of state variable theory is that the response of a system may be specified in terms of its initial conditions at any instant of time and its inputs from that time on. The n initial conditions, or numbers are called state variables. The state variables used for a specific problem are not unique and may be chosen in many different ways. Information known about the system and experience in handling the resulting equations usually dictate the choice of state variables (11).

Linear systems may be represented by the following system of equations:

$$\frac{dx_i}{dt} = \sum_{j=1}^n a_{ij} x_j + \sum_{j=1}^m b_{ij} r_j, \quad (i = 1, 2, 3, \dots, n), \quad m \leq n, \quad (2.1)$$

$$y_i = \sum_{j=1}^n c_{ij} x_j, \quad (i = 1, 2, 3, \dots, r), \quad r \leq n, \quad (2.2)$$

where a_{ij} , b_{ij} , and c_{ij} are constants, the r_j 's are inputs, the x_j 's are state variables, and the y_i 's are outputs. In matrix notation

$$\dot{\underline{X}} = \underline{A} \underline{X} + \underline{B} \underline{R}, \quad (2.3)$$

$$\underline{Y} = \underline{C} \underline{X}, \quad (2.4)$$

where \underline{X} is a column matrix, and $\dot{\underline{X}}$ is a column matrix whose elements are the derivatives of the state variables, \dot{x}_1, \dot{x}_2 , etc. \underline{A} is an $n \times n$ matrix whose elements are the coefficients a_{ij} . \underline{B} is an $n \times m$ matrix whose elements are the coefficients b_{ij} , and \underline{C} is an $r \times n$ matrix whose elements are c_{ij} . \underline{Y} is a column matrix of outputs, y_1, y_2 , etc., and \underline{R} is a matrix of inputs, r_1, r_2 , etc. For a time-varying, nonlinear system, the equations would be

$$\frac{dx_i}{dt} = \sum_{j=1}^n a_{ij}(x_1, x_2, \dots, x_n, t) x_j + \sum_{j=1}^m b_{ij}(x_1, x_2, \dots, x_n, t) r_j \quad (2.5)$$

$$y_i = \sum_{j=1}^n c_{ij}(x_1, x_2, \dots, x_n, t) x_j \quad (2.6)$$

and in matrix notation

$$\dot{\underline{X}} = \underline{A}(f(\underline{X}), t) \underline{X} + \underline{B}(g(\underline{X}), t) \underline{R} \quad (2.7)$$

$$\underline{Y} = \underline{C}(h(\underline{X}), t) \underline{X}, \quad (2.8)$$

where the functions $f(\underline{X})$, $g(\underline{X})$, and $h(\underline{X})$ are scalar, algebraic expressions composed of the scalar elements of the column matrix \underline{X} .

If the Laplace transform of Equation 2.3 is taken, the result is:

$$s \underline{X}(s) - \underline{X}(0^+) = \underline{A} \underline{X}(s) + \underline{B} \underline{R}(s), \quad (2.9)$$

where, s = Laplace transform variable, $\underline{X}(s)$ = column matrix whose elements are the Laplace transforms of the state variables, $\underline{R}(s)$ = column matrix whose elements are the Laplace transforms of the inputs. Rearranging, and performing matrix algebra,

$$\underline{X}(s) = [s\underline{I} - \underline{A}]^{-1} \underline{X}(0^+) + [s\underline{I} - \underline{A}]^{-1} \underline{B} \underline{R}(s),^* \quad (2.10)$$

where \underline{I} is the unit matrix. Taking the inverse Laplace transform

$$\underline{X}(t) = \mathcal{L}^{-1} \left\{ [s\underline{I} - \underline{A}]^{-1} \right\} \underline{X}(0^+) + \int_0^t \mathcal{L}^{-1} \left\{ [s\underline{I} - \underline{A}]^{-1} \right\}_{t=\tau} \underline{B} \underline{R}(t-\tau) d\tau. \quad (2.11)$$

Substituting

$$\underline{\phi}(t) = \mathcal{L}^{-1} \left\{ [s\underline{I} - \underline{A}]^{-1} \right\} \quad (2.12)$$

gives

$$\underline{X}(t) = \underline{\phi}(t) \underline{X}(0^+) + \int_0^t \underline{\phi}(\tau) \underline{B} \underline{R}(t - \tau) d\tau. \quad (2.13)$$

* $[s\underline{I} - \underline{A}]^{-1}$ denotes the inverse of $[s\underline{I} - \underline{A}]$.

Thus, if t_n represents the time 0^+ in Equation 2.13 and t_{n+1} represents t ,

$$\underline{X}(t_{n+1}) = \underline{\phi}(t_{n+1} - t_n) \underline{X}(t_n) + \int_{t_n}^{t_{n+1}} \underline{\phi}(\tau) \underline{B} \underline{R} (t_{n+1} - \tau) d\tau. \quad (2.14)$$

Equation 2.14 translates the state variables from their values at time t_n to new values at time t_{n+1} . The elements of the $\underline{\phi}(t_{n+1} - t_n)$ matrix can change from one iteration interval to the next as long as they are constant within each interval. This is a property which will be used in later problems.

A careful inspection of Equations 2.13 and 2.14 reveals that the only unknown quantity is the matrix $\underline{\phi}(t)$ and Equation 2.12 defines it as the inverse Laplace transform of the matrix $[sI - A]^{-1}$. Although this is a straightforward approach for finding the $\underline{\phi}(t)$ matrix, there are other methods of finding this matrix from inspection of diagrams which represent the system to be analyzed (11).

The method used in this report, other than the straightforward approach, is discussed in an article by Kalman and Bertram (20) and is based on the general analog computer simulation of Figure 1. It is important to observe that this simulation represents the system with no inputs connected. To evaluate the $\underline{\phi}(t)$ matrix let;

$g_{ij}(s)$ = transfer function from the input of the j^{th} integrator to the output of the i^{th} integrator in the analog simulation of Figure 1.

Then,

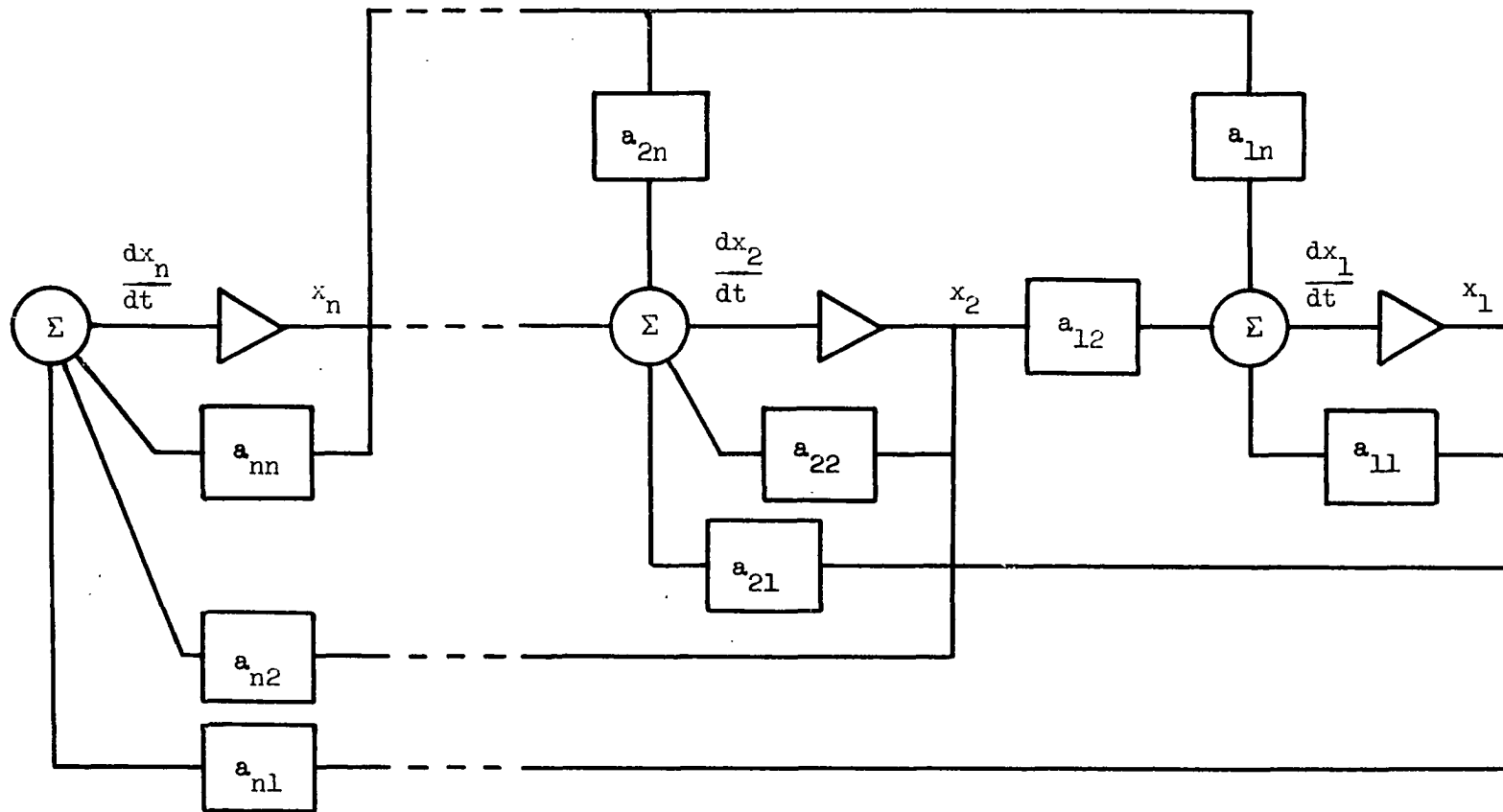


Figure 1. Analog simulation for a system of first order differential equations (1/, Figure 3)

$$\phi(t) = \mathcal{L}^{-1} \begin{bmatrix} g_{11}(s) & g_{1n}(s) \\ g_{n1}(s) & g_{nn}(s) \end{bmatrix}, \quad (2.15)$$

where the inverse Laplace transformation, \mathcal{L}^{-1} , is applied to each element of the matrix separately. This method is used in Appendix A to simulate a model proposed by M. Clynes for respiratory sinus arrhythmia (7).

There are both advantages and disadvantages of using this type of system formulation and a discussion of some of the properties of state variable equations will follow. Since the type of system studied will certainly influence the choice of method of analysis, this discussion will refer to typical systems present in body control mechanisms.

Since the state variable matrix equations can be programmed on a digital computer, which also can be given further instructions as to how to compute the desired results, it is possible to have precise control of all transfer functions as well as the parameters within the transfer functions. This advantage will be illustrated in the simulation of M. Clynes' model, where a transfer function changes form depending on the derivative of its input variable. Due to this flexibility of equations and parameters, this method is ideally suited to handle large systems with parameters and transfer functions varying in a prescribed fashion. This is helpful in descriptions of complex body functions such as blood pressure regulation.

The most obvious disadvantages of the state variable approach are the need for a digital computer for rapid analysis and the difficulty, as compared to an analog computer, in changing fixed parameters during

simulation runs. Even a system of two variables becomes cumbersome at times when long-hand calculations are made and a digital computer is certainly welcome. Yet, even if programs are available and can be used for the specific problem to be solved, it is difficult to change individual parameters in the model in order to assess their influence on the final answer. Hopefully, these disadvantages are outweighed by the greater mathematical flexibility offered by the formulation.

III. LIAPUNOV'S SECOND METHOD APPLIED TO A NONLINEAR BIOLOGICAL SYSTEM

A. Introduction

In the study of control systems in general, there are two separate goals which may be achieved. One goal is to find the actual variation, as a function of time, of all the variables concerned; however, in many problems this is difficult, if not impossible, with present methods. To gain more information about these difficult problems, a different approach is attempted. The information from this approach being facts concerning the solutions but not the actual solutions themselves. This second approach will be used in this chapter since the system to be analyzed is nonlinear and its time solution is not easily obtained by conventional methods.

The chapter will begin with a brief description of the cardiac pacemaker or sinoatrial node and the influence of vagal innervation on its rate. Then Liapunov's Second Method will be discussed and later used to predict the upper limit for vagal tone or impulse frequency above which the sinoatrial node ceases to be active.

B. Mathematical Description of Sinoatrial Node Influence on Heart Rate

The cardiac pacemaker or sinoatrial node is located near the junction of the precava and right atrium. It is club shaped in the dog and tapers to a fine end, or tail, at the angle of the junction of the precava and the postcava (12). Nearly any region of the syncytial tissue of cardiac muscle can produce propagating action potentials but the sinoatrial node region seems to control the actual heart rate because it develops action potentials faster than any other part of the heart muscle. The potentials of this region are never static, i.e., during diastole the

potentials are falling until a definite voltage level is reached, then another impulse is generated and propagated away through the cardiac muscle. This causes the atrium to contract, and the action potential propagates to the atrioventricular node which then responds to send impulses through the Purkinje conduction system. This causes the ventricles to contract and force blood out of the heart. The repetition rate of this cycle is controlled principally by the sinoatrial node but in its absence the atrioventricular node will take over. The main interest of this study is in the functional properties of the sinoatrial node and the effect of vagal influence on them.

Warner and Cox (38) have suggested a mathematical model which relates frequency of vagal stimulation to the period of heart rate governed by the pacemaker. Their model, shown diagrammatically in Figure 2, relies on the fact that acetylcholine is the chemical mediator which controls the rate of pacemaker potential variations. The following equations mathematically describe their interpretation of the time variation of the heart rate. The word Equations 3.1a and 3.2a are added by the author for clarity.

$$\begin{array}{l} \text{The rate of change} \\ \text{of charged vesicles} \end{array} = \begin{array}{l} \text{The increase of} \\ \text{charged vesicles} \end{array} - \begin{array}{l} \text{The decrease of} \\ \text{charged vesicles} \end{array} \quad (3.1a)$$

$$\frac{dN(t)}{dt} = k_7(N_m - N(t)) - k_8 N(t) f_2 \quad (3.1b)$$

$$\begin{array}{l} \text{The rate of change} \\ \text{of acetylcholine at} \\ \text{the sinoatrial node} \end{array} = \begin{array}{l} \text{Amount of acetylcholine} \\ \text{released by action} \\ \text{potentials} \end{array} - \begin{array}{l} \text{Amount of} \\ \text{acetylcholine} \\ \text{hydrolyzed} \end{array} \quad (3.2a)$$

$$2b \quad \frac{dC_2(t)}{dt} = \frac{k_8 n C_1 N(t) f_2}{V_2} - \frac{k_9}{V_2} C_2(t) \quad (3.2b)$$

The equation describing the period, p , of heavy activity is

$$3 \quad p = p_0 + k_{10} C_2(t), \quad \text{for } C_2(t) < C_s, \quad (3.3)$$

where p_0 is the initial period of the heart cycle before stimulation and k_{10} is a proportionality constant.

Their reasoning and explanation of these equations is as follows

(38):

"At the end of each nerve fiber there are small vesicles which contain acetylcholine in concentration C_1 . A fraction k_8 of these vesicles discharge acetylcholine with the arrival of each stimulus. The rate at which the number N of these vesicles (which are "charged" with acetylcholine and are capable of discharging) changes with respect to time is shown in Equation 3.1b. N_m is a constant and represents the maximum number of charged vesicles achieved in a steady state when the nerve is not firing. With each action potential $k_8 N(t)$ vesicles are discharged from each nerve ending decreasing the number of charged vesicles. The rate at which the number of charged vesicles is replenished is proportional to the difference between $N(t)$ and N_m , that is, at a rate proportional to the amount by which $N(t)$ is decreased from its resting value due to preceding action potentials. $C_2(t)$, the concentration of acetylcholine at the sinoatrial node just outside the vesicle near the nerve ending, is described by Equation 3.2b."

As shown in Equation 3.2b, the concentration $C_2(t)$ will change at a rate which depends on $f_2(t)$, and the product $k_8 C_1 N(t)$, which is the amount of acetylcholine released by each action potential, and on n , the number of fibers responding to each stimulus. The acetylcholine is hydrolyzed by the enzyme cholinesterase at a rate proportional to $C_2(t)$. V_2 is the volume into which the ejected acetylcholine is diluted. The period p of the heart cycle will be changed by an amount proportional to $C_2(t)$ as

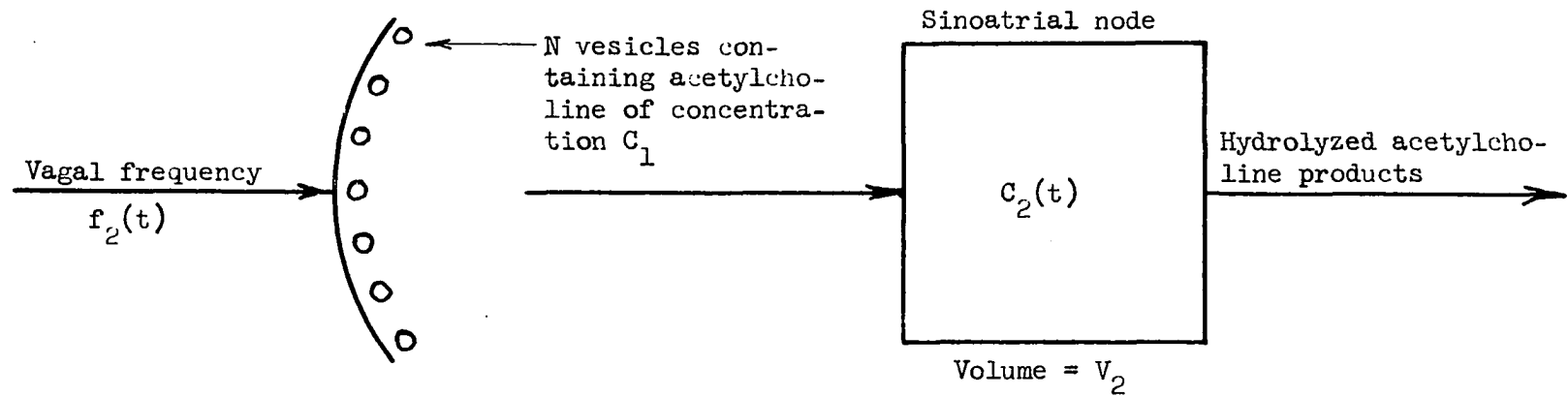


Figure 2. Schematic diagram of the proposed mechanism of discharge and hydrolysis of acetylcholine at the sinoatrial node (38)

long as $C_2(t)$ does not exceed a critical value C_s .

Warner and Cox have assumed a linear hydrolysis of acetylcholine in their model and have restricted the model to values of $C_2(t)$ lower than some constant C_s . Since the hydrolysis of acetylcholine is an enzymatic reaction, it is reasonable to assume a linear rate of reaction with respect to substrate concentration when the substrate is present in much lower concentration than the enzyme. When the substrate concentration becomes appreciable and the enzyme is being taxed to its capacity, a saturation will occur and no matter how much substrate is added only a constant amount will be hydrolyzed (10). This is shown by the smooth curve in Figure 3. Warner and Cox did not pursue their model any further than the linear approximation for the enzyme reaction, but did specify an upper limit of $C_2(t) = C_s$ above which their equations did not hold. They also reported sinoatrial block for vagal stimulation frequencies above 13 to 15 cycles per second.

This report will show that the block can be predicted if the assumed enzyme reaction is described by a reaction curve similar to the smooth curve of Figure 3. This function is represented mathematically as:

$$- \frac{d C_2(t)}{dt} = \frac{k_9 C_s}{V_2} \frac{C_2(t)}{K_m + C_2(t)} \quad (3.4)$$

This is the well known Michaelis-Menten equation (10, p. 252) which describes the rate of decomposition of a substrate, $C_2(t)$, in the presence of an enzyme. K_m is the Michaelis constant and is dependent on the ability of the enzyme to influence the decomposition. The quantity $\frac{k_9 C_s}{V_2}$ is the maximum rate of reaction possible.

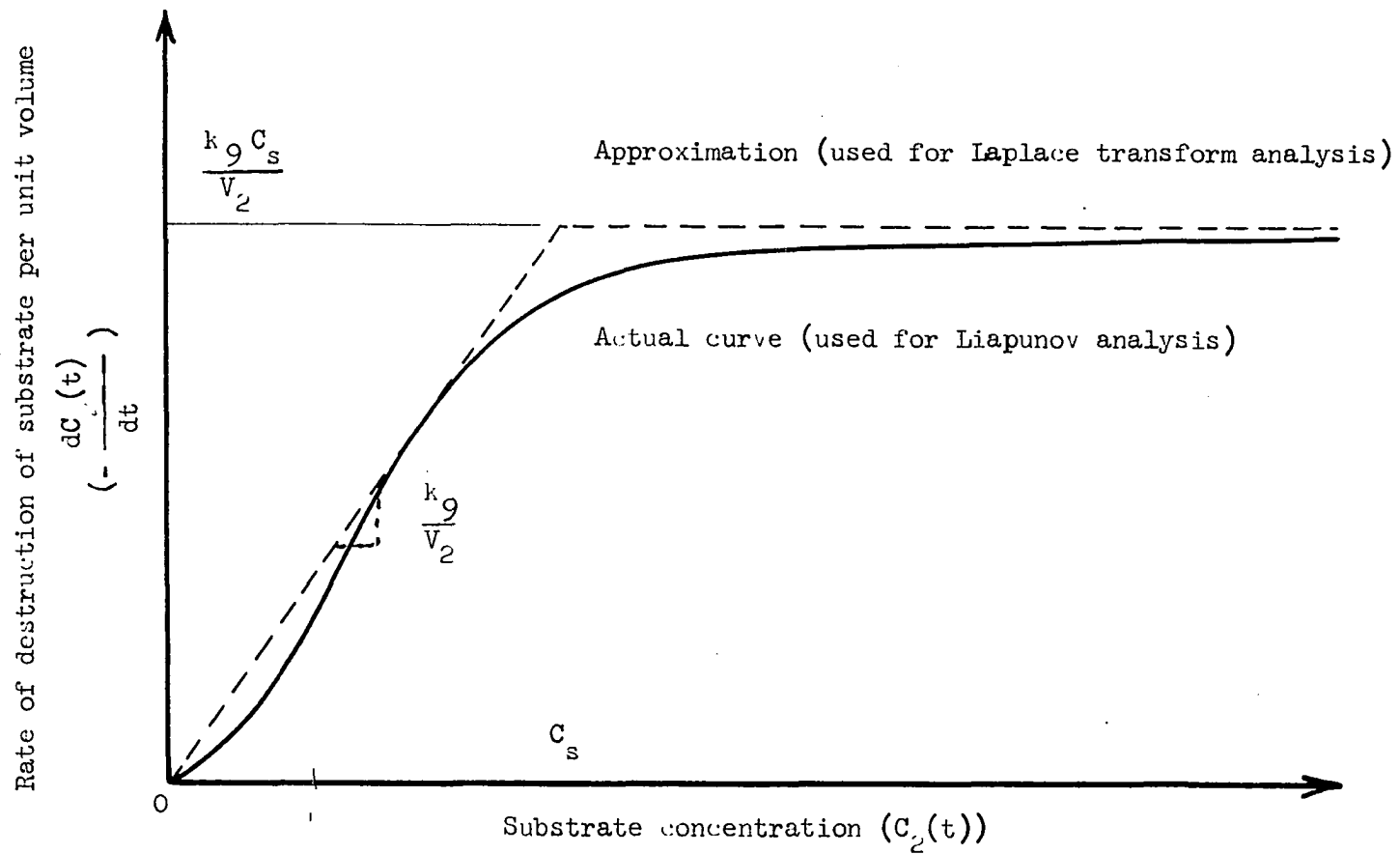


Figure 3. The rate of destruction of a substrate as a function of the concentration of the substrate

The straight line approximation to this curve, shown as a dotted line in Figure 3, is used in Appendix B to facilitate a Laplace transform analysis of this problem.

Because of the lack of knowledge of the mechanics of reaction within the node, the saturation characteristic cannot be attributed to enzyme scarcity only, but may be due to several other factors, such as diffusion of acetylcholine to the enzyme sites (38), degeneration of the enzyme, or other unknown intermediary reactions. Although the exact mechanism is not known and therefore the foregoing formulation has not been substantiated experimentally, this formulation is similar to the one proposed by Warner and Cox in the low concentration range and also predicts sinoatrial block at high frequencies of stimulation.

Substituting the proposed hydrolysis function into Equation 3.2b and rearranging Equation 3.1b, the following system of equations results:

$$\frac{dN(t)}{dt} = -(k_7 + k_8 f_2) N(t) + k_7 N_m \quad (3.5)$$

$$\frac{dC_2(t)}{dt} = \frac{n k_8 C_1 f_2}{V_2} N(t) - \frac{k_9 C_s}{V_2} \frac{C_2(t)}{K_m + C_2(t)} \quad (3.6)$$

This is the system which will be analyzed by using results from Liapunov's Second Method (23). Before applying this theory to the problem, a number of theorems and definitions will be presented.

C. Liapunov's Second Method

The system to be considered will be of the form shown in the following equation:

$$\dot{\underline{X}} = \underline{F}(\underline{X}, t), \quad (3.7)$$

where $\dot{\underline{X}}$ is a column matrix of derivatives of state variables mentioned in Chapter II. $\underline{F}(\underline{X}, t)$ is a column matrix whose independent variables are the state variables and time. The method of Liapunov is concerned with the behavior of a scalar function $V(\underline{X})$ which is called the Liapunov function. This function must have the following properties (22),

- (a) $V(\underline{X})$ is continuous together with its first partial derivatives in a certain open region Ω about the origin, where Ω is the region in which the inequality, $\underline{X} < A$, is satisfied.
- (b) $V(0) = 0$
- (c) Outside the origin (and always in Ω) $V(\underline{X})$ is positive
- (d) $\frac{dV(\underline{X})}{dt} \leq 0$

Property c implies that $V(\underline{X})$ is non-negative and vanishes only at the origin. A helpful geometric interpretation of $V(\underline{X})$ is given by LaSalle and Lefschetz (22) in their book on Liapunov's Second Method from which the introductory material of this chapter is taken.

In the introductory discussion which follows, a number of terms and concepts are used which must be defined and explained. These terms will now be defined. Figure 4 is included as an aid in interpreting these definitions.

1. The origin shall be the point $V(0) = 0$.
2. $S(R)$ is the region $\underline{X} < R$
3. $H(R)$ is the boundary $\underline{X} = R$
4. The annular region $r \leq \underline{X} \leq R$ shall be written S_r^R

5. \underline{X}^0 shall be the initial starting conditions for the vector \underline{X} and the subsequent unique path followed as time advances will be denoted by g^+ .
6. The origin is stable whenever for each $R < A$ there is an $r \leq R$ such that if a path g^+ initiates at a point \underline{X}^0 of the spherical region $S(r)$ it remains in the spherical region $S(R)$ ever after; that is, a path starting in $S(r)$ never reaches the boundary sphere $H(R)$ of $S(R)$ in Figure 4.
7. The origin is unstable whenever for some R and any r , no matter how small, there is always in the spherical region $S(r)$ a point \underline{X} such that the path g^+ through \underline{X} reaches the boundary sphere $H(R)$.

It is important to observe that these definitions of stability concern the origin, $F(0,t) = 0$. Therefore, it is sometimes necessary to translate the origin by the transformation,

$$\underline{X}' = \underline{X} - \underline{a}. \quad (3.8)$$

Liapunov's theorems for stability are as follows:

Theorem 1. If,

$$(a) \quad V(\underline{X}) > 0 \quad \text{for} \quad V(\underline{X}) < \epsilon$$

$$(b) \quad \dot{V}(\underline{X}) > 0 \quad \text{for all } \underline{X} \text{ in } \Omega$$

\Rightarrow the origin is unstable

Theorem 2. If,

$$(a) \quad V(\underline{X}) > 0 \quad \underline{X} \neq 0$$

$$(b) \quad \dot{V}(\underline{X}) \leq 0 \quad \text{for all } \underline{X} \text{ in } \Omega$$

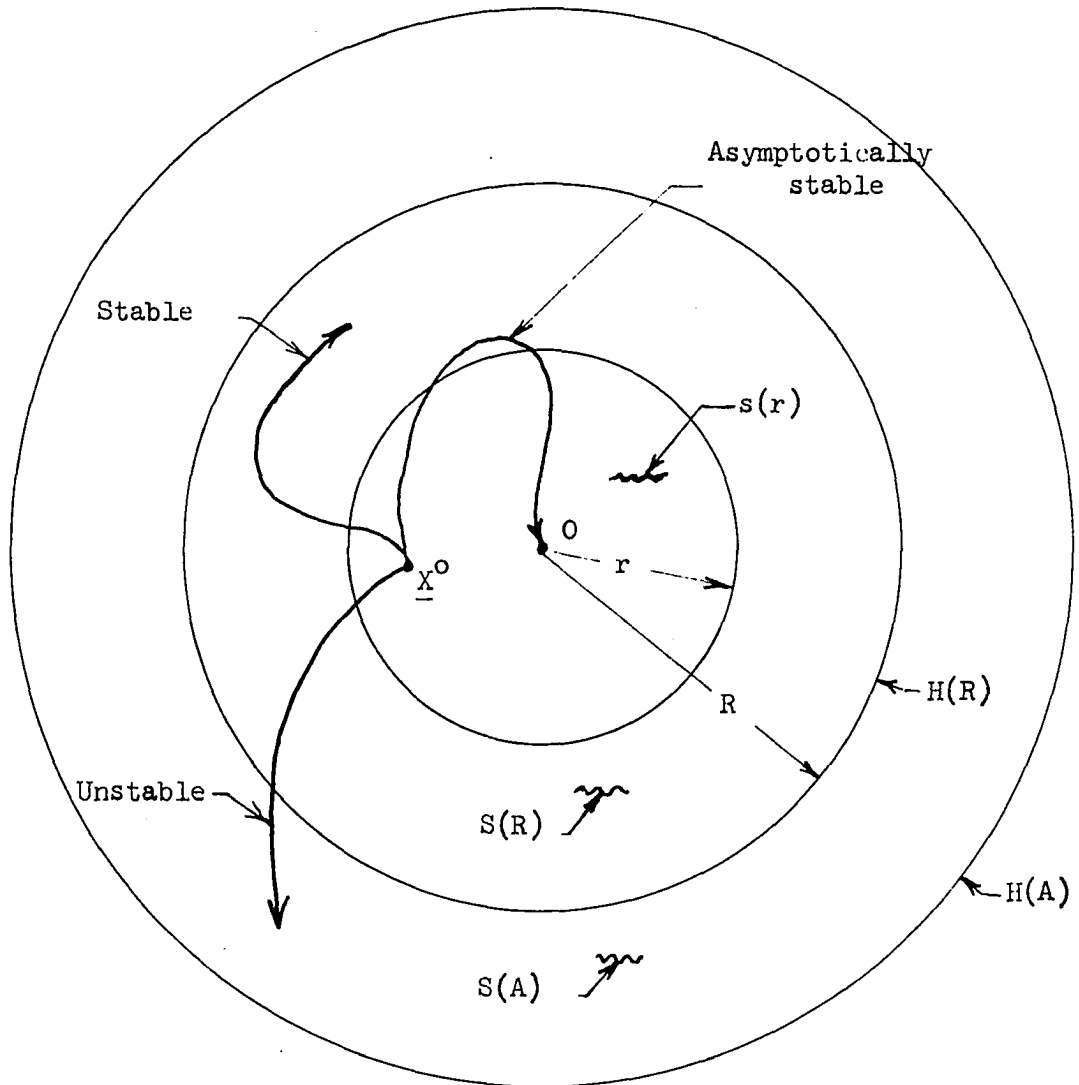


Figure 4. Illustration of the terms associated with the various degrees of stability (20, p. 31)

\Rightarrow the origin is stable

Theorem 3. If,

$$(a) \quad V(\underline{X}) > 0 \quad \underline{X} \neq 0$$

$$(b) \quad \dot{V}(\underline{X}) < 0 \quad \underline{X} \neq 0$$

\Rightarrow the origin is asymptotically stable

Inspection of these theorems shows that the theorem concerning asymptotic stability is the most useful, in terms of knowing how the variables are behaving or will behave in the future.

The greatest disadvantage of this approach is the formulation of $V(\underline{X})$. There is no unique method by which $V(\underline{X})$ can be constructed from knowledge of the system equations. This is an active area of research at the present time and hopefully a method will soon be discovered.

Since the $V(\underline{X})$ is not unique, the conditions for stability associated with a specific $V_i(\underline{X})$ can only be classified as necessary and not sufficient. It is possible that another Liapunov function $V_f(\underline{X})$ would yield more general conditions than the initial $V_i(\underline{X})$. Thus throughout the use of this theory, it must be kept in mind that all criteria are only necessary conditions and not sufficient.

Despite the difficulty in forming satisfactory Liapunov functions many systems have been investigated by Liapunov's Second Method and useful results gleaned from the work. In the investigation of some nonlinear systems, this method has produced stronger conditions than the Routh-Hurwitz criteria (29). Krasovskii (21) has found this to be true for many systems consisting of two differential equations. Higher order systems have not been completely investigated because of the much greater mathematical complexity, but work is being done in this area (14, p. 47).

A system of equations analogous to that which will be discussed later in connection with the heart rate control system is analyzed in Hahn's (14) book on Liapunov's Second Method. The system of equations is:

$$\frac{dy}{dt} = ay + cx \quad (3.9)$$

$$\frac{dx}{dt} = by + f(x) \quad (3.10)$$

The Liapunov function used to derive necessary conditions for asymptotic stability is

$$v(x,y) = \int_0^x (f(\xi) a - bc \xi) d\xi + \frac{1}{2} (ax - by)^2.$$

Using this function, the following conditions are necessary for asymptotic stability from any initial point (x,y) (14, p. 43).

$$\text{Condition 1. } \left(\frac{f(x)}{x} + a \right) < 0 \quad x \neq 0$$

$$\text{Condition 2. } \left(\frac{a f(x)}{x} - bc \right) > 0 \quad x \neq 0$$

If these conditions are true for the system of Equations 3.9 and 3.10, the values of x and y will tend to zero from any starting point (x,y) as time approaches infinity.

This concludes the discussion of Liapunov's theory and the theoretical results to be used in the next section. The next section will deal with the application of these results to the pacemaker control problem. The result wanted is a condition specifying that value of vagal stimula-

tion frequency produces infinitely growing values of $C_2(t)$ or instability.

D. Application of Liapunov's Second Method

to the Sinoatrial Node Equations

The equations of interest are Equations 3.5 and 3.6. For convenience, the following substitutions are made:

$$A = k_7 + k_8 f_2, \quad B = k_7 N_m, \quad C = \frac{n k_8 C_1 f_2}{V_2}$$

and

$$D = \frac{k_9 C}{V_2} .$$

With these substitutions, Equations 3.5 and 3.6 become

$$\frac{dN(t)}{dt} = -A N(t) + B \quad (3.11)$$

and

$$\frac{dC_2(t)}{dt} = C N(t) - \frac{D C_2(t)}{K_m + C_2(t)} . \quad (3.12)$$

The purpose of this section is to investigate the conditions necessary for stability of this system of equations. First, it is necessary to perform a linear transformation of Equations 3.5 and 3.6 in order to satisfy the condition stated on page 19,

$$F(\underline{X}, t) \quad \left| \begin{array}{l} = 0 \\ \underline{X} = 0 \end{array} \right. .$$

For our set of equations, this will be satisfied if

$$N'(t) = N(t) - \frac{B}{A} \quad (3.13)$$

and

$$C_2'(t) = C_2(t) - \frac{K_m}{\frac{AD}{CB} - 1} \quad (3.14)$$

With this transformation,

$$\frac{dN'(t)}{dt} = -A N'(t) \quad (3.15)$$

and

$$\frac{dC_2'(t)}{dt} = C N'(t) + \frac{CB}{A} - D \cdot \frac{C_2'(t) + \frac{K_m}{\frac{AD}{CB} - 1}}{K_m + C_2'(t) + \frac{K_m}{\frac{AD}{CB} - 1}} \quad (3.16)$$

These equations are now in a form analogous to Equations 3.9 and 3.10

where, identifying analogous terms,

$$a = -A, \quad b = C, \quad c = 0, \quad \text{and}$$

$$f(x) = f(C_2'(t)) = \frac{CB}{A} - D \cdot \frac{C_2'(t) + \frac{K_m}{\frac{AD}{CB} - 1}}{K_m + C_2'(t) + \frac{K_m}{\frac{AD}{CB} - 1}} \quad (3.16)$$

In order to find the necessary conditions for asymptotic stability of Equations 3.15 and 3.16, Conditions 1 and 2 for asymptotic stability of Equations 3.9 and 3.10 are analyzed with the proper substitutions used. To satisfy Condition 1,

$$\frac{f(C_2'(t))}{C_2'(t)} < A, \quad (3.17)$$

and for Condition 2,

$$\frac{f(C_2'(t))}{C_2'(t)} < 0. \quad (3.18)$$

Since if Condition 2 is satisfied Condition 1 will also be satisfied, the necessary conditions for asymptotic stability can be found from the consideration of inequality 3.18. Therefore, substituting the proper expression for $f(C_2'(t))$, it is evident that, for asymptotic stability, the inequality

$$\frac{1}{C_2'(t)} \left[\frac{CB}{A} - D \frac{C_2'(t) + \frac{K_m}{\frac{AD}{CB} - 1}}{K_m + C_2'(t) + \frac{K_m}{\frac{AD}{CB} - 1}} \right] < 0, \quad C_2'(t) \neq 0, \quad (3.19)$$

must be satisfied. In order to find the necessary conditions for stability for the original system, $C_2'(t)$ is replaced with its equivalent expression obtained from Equation 3.14. Then

$$\left[\frac{1}{C_2(t) - \frac{K_m}{\frac{AD}{CB} - 1}} \right] \left[\frac{CB}{A} - D \frac{C_2(t)}{K_m + C_2(t)} \right] < 0. \quad (3.20)$$

Multiplying and clearing fractions within each term,

$$\left[\frac{AD - CB}{(AD - CB)C_2(t) - CB K_m} \right] \left[\frac{-((AD - CB)C_2(t) - CB K_m)}{A(K_m + C_2(t))} \right] < 0. \quad (3.21)$$

Multiplying by (-1) and reversing the inequality,

$$\frac{(AD - CB)((AD - CB)C_2(t) - CB K_m)}{A(K_m + C_2(t))((AD - CB)C_2(t) - CB K_m)} > 0. \quad (3.22)$$

Therefore, for asymptotic stability

$$\frac{AD}{A(K_m + C_2(t))} > \frac{CB}{A(K_m + C_2(t))} \quad (3.23)$$

must be true. The quantity $(K_m + C_2(t))$ may be either positive or negative and the criteria that must be satisfied are

$$AD > CB \quad \text{for} \quad C_2(t) > -K_m \quad (3.24)$$

$$AD < CB \quad \text{for} \quad C_2(t) < -K_m. \quad (3.25)$$

Since the concentration $C_2(t)$ cannot physically be negative, the only criterion in this specific problem is inequality 3.24. Inserting the

proper values for A, B, C, and D gives

$$\frac{k_9 C_s}{V_2} > \frac{k_7 k_8 N_m n C_1 f_2}{(k_7 + k_8 f_2) V_2} \quad (3.26)$$

for $C_2(t) > 0 > -K_m$. Rearranging terms in inequality 3.16, the stability criteria for f_2 is found to be

$$f_2 < \frac{C_s}{\frac{k_8 N_m n C_1}{k_9} - \frac{k_8 C_s}{k_7}} \quad (3.27)$$

Rearranging the right hand side of inequality 3.27 results in the conclusion that for the concentration of acetylcholine to approach a constant value as time approaches infinity, the frequency, f_2 , of vagal stimulation must be less than the quantity,

$$\frac{k_9 C_s k_7}{k_7 k_8 N_m n C_1 - k_8 k_9 C_s}.$$

This implies that if $k_9 C_s$ is increased, the upper limit on $f_2(t)$ which insures stability, should also increase. If $k_9 C_s$ is decreased the upper limit on f_2 should decrease. Since the drug atropine combines with the receptor sites of the sinoatrial end plates (5, p. 688), it is postulated that this phenomenon will effectively increase $k_9 C_s$. The reason for this being that, since atropine is combining with the receptor sites, this reaction effectively lowers the concentration of acetylcholine near the sites as long as the drug is present.

Since physostigmine competes with acetylcholine for the enzyme cholinesterase (5, p. 688), it is postulated that the addition of this drug will decrease k_9 thus decreasing $k_9 C_s$. This raises the concentration of acetylcholine at the receptor sites and lowers the stimulation frequency limit for stability.

If the piecewise continuous curve of Figure 3 is used to describe the decomposition of $C_2(t)$, the Equations 3.5 and 3.6 can be investigated by Laplace transform methods as in Appendix B. It is interesting to note the close agreement between the two approaches as far as stability conditions are concerned.

IV. EXPERIMENTAL VERIFICATION OF PACEMAKER ANALYSIS

Twelve mongrel dogs, male and female, were anesthetized with sodium-pentobarbital (30 mg/kg), supplemented as needed. An endotracheal tube was inserted and the animals maintained on positive pressure ventilation with 100% oxygen. In order to isolate both left and right vagi, a mid-line incision was made from the base of the larynx, caudad to the manubrium sterni cartilage. The common carotid arteries and their respective vagi were exposed by separating the sternocephalicus and sternohyoideus muscles. Each vagus nerve was dissected out of the carotid sheath and severed at the level of the first tracheal cartilage. The distal ends were connected by means of sleeve electrodes to a Grass S-4 stimulator equipped with a Grass SIU-4B isolation unit. The stimulus was of one millisecond duration and from 20 to 40 volts amplitude depending on maximal response of heart rate to stimulation at various frequencies. After maximal response was achieved, the voltage was held constant at the level throughout the experiment on each dog. The frequency was varied in calibrated steps of 1,2,4,7.6,10,12.5,13.3,15, and 20 cycles per second. If data points were needed in between these readings less accurate frequency values were used.

In order to expose and locate the pacemaker, the chest was opened through the right, fifth intercostal space and rib retractors used to spread the ribs for access to the right atrium. The cardiac lobe of the lung was retracted dorsad exposing the right atrium. The pericardial sac was incised parallel and ventrad to the phrenic nerve and, using tissue forceps, the cut edges were retracted dorsad and ventrad to expose the junction of the right atrium and the precava. The sinoatrial node was

located by selectively dropping ice water on circumscribed areas of the right atrium. The point at which this procedure caused a slowing of heart rate was recognized as the sinoatrial node (33). This was usually near and slightly caudal to the junction of the right atrium and the precava.

All recordings were monitored on the Grass Model 5 Polygraph. An electrocardiogram, lead II, was recorded as well as one with a special lead arrangement which enhanced the P wave of a normal electrocardiogram. This was done because the P wave potential is composed mainly of contributions from electrical activity in the sinoatrial region. The entire system is illustrated in Figure 5. An insulated wire with a bead of solder on the end was passed into the jugular vein at the level of the first tracheal ring and the bead passed to the precava region just cranial to the right atrium. A reference electrode was attached to the medial portion of the cranium and a common ground placed on the right hind leg. Figures 6 and 7 show the recordings taken for two different frequencies of stimulation. Figure 6 shows the response to a frequency of stimulation which did not produce sinoatrial block. The upper record, from the special P wave monitoring arrangement, shows a strong P wave (the initial large spike of each two-spike complex) present during stimulation. Figure 7 shows the response to a frequency which did produce sinoatrial node block. The P wave of both the top and bottom record disappears during stimulation.

Each experiment consisted of a control run of heart rate recordings as the frequency was varied from zero to the point at which the P wave disappeared for at least 10 seconds. Each succeeding run was exactly the

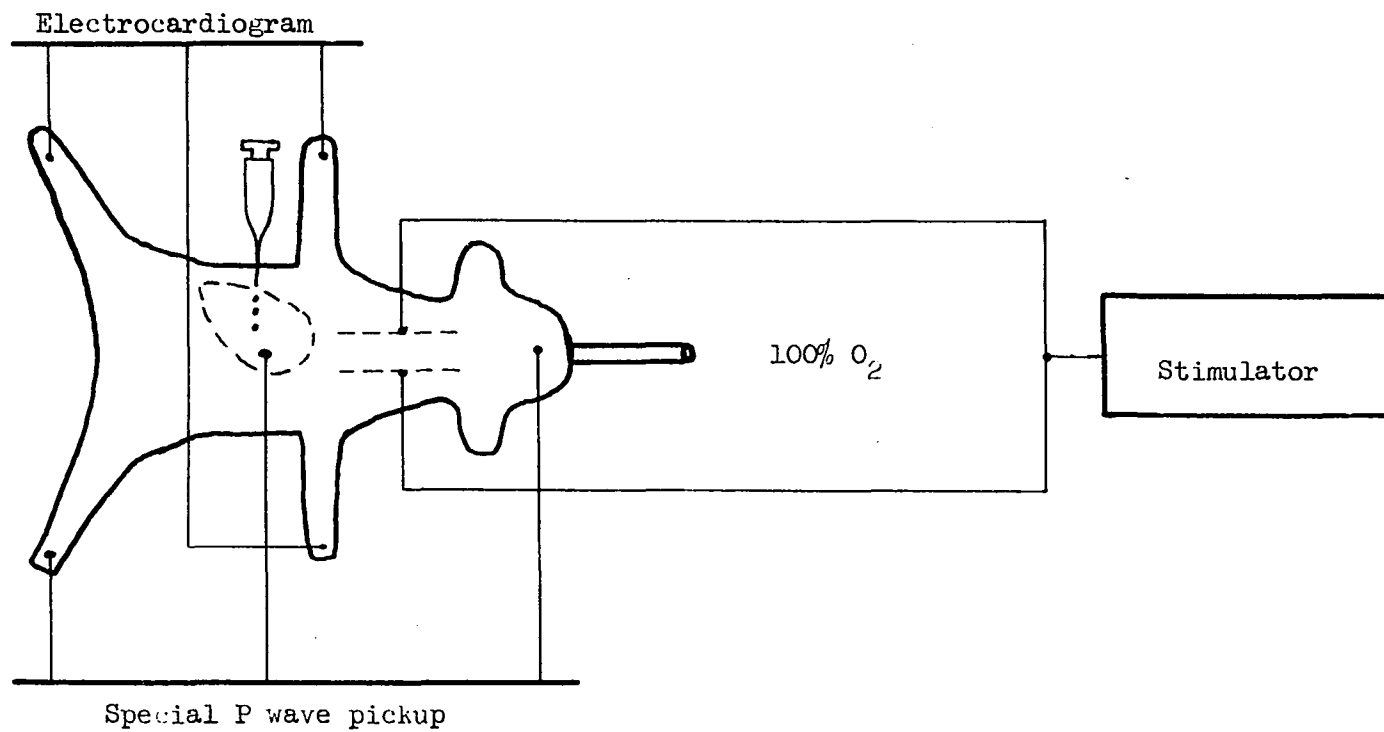
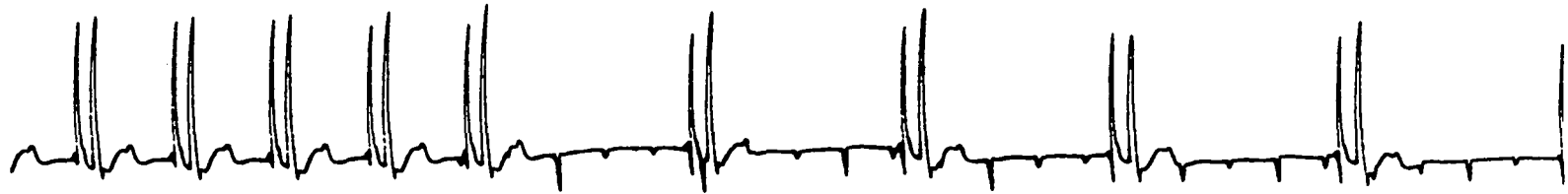


Figure 5. Experimental arrangement for vagal stimulation

472



P wave channel



EKG

1 second

stimulation



Figure 6. Heart rate response to vagal stimulation (frequency of stimulation; 4 cycles per second, intensity; 40 volts, chemical influence, 6 drops of 5µg/cc physostigmine)

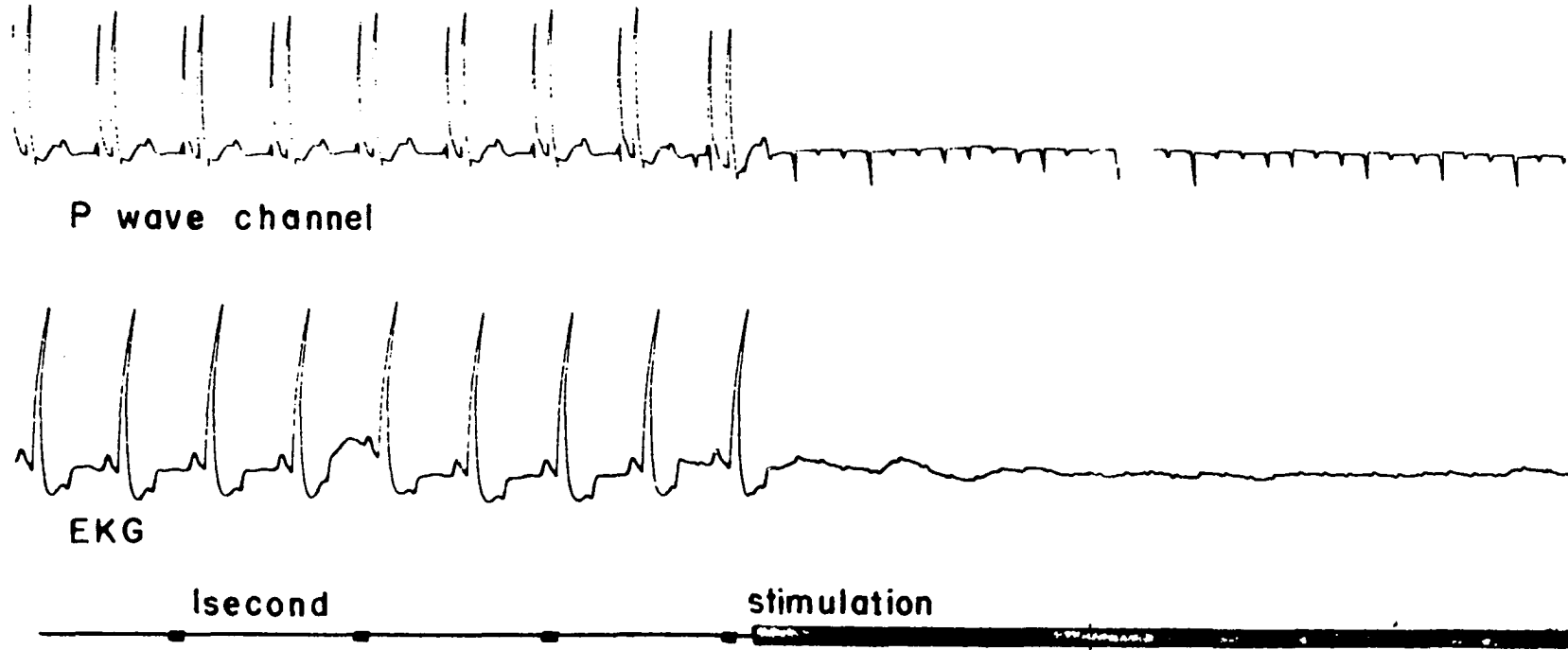


Figure 7. Heart rate response to vagal stimulation (frequency of stimulation; 8 cycles per second, intensity; 40 volts, chemical influence, 6 drops of 5 μ g/cc physostigmine)

same except for local administration of either atropine or physostigmine on the sinoatrial node just prior to making the run. At each frequency of stimulation the heart rate was allowed to reach a steady value before the rate was used as a data point. The results of a typical experiment are shown in Figures 8 and 9. The heart rate of all dogs tested reacted in qualitatively the same manner; i.e., if physostigmine was added, the resulting frequency limit was lowered and if atropine was added the limit was raised.

Atropine and physostigmine were administered drop by drop through a 20 gauge needle and the concentration of both drugs was $5\mu\text{gm}/\text{cc}$. As shown in Figure 8, physostigmine was added first in 3 drop increments. As shown in Figure 9, atropine was then added in 2 drop increments. Individual experiments on the effect of atropine and physostigmine alone were performed and similar responses recorded. Each of the curves of Figures 8 and 9 can be reproduced faithfully for 30 to 45 minutes after the administration of the drug on the sinoatrial node. The total time required to obtain the data for the entire series of curves plotted in Figure 8 and 9 was approximately 20 minutes. Thus, it was assumed that the influence of each incremental addition of drug remained for the duration of each experiment.

Figures 8 and 9 illustrate the predicted influence, which was postulated in Chapter III, when the sinoatrial node is perfused with physostigmine or atropine. In both cases, the predictions were substantiated in a qualitative sense. These results are encouraging in that they further substantiate the model proposed for the sinoatrial node. Since this was

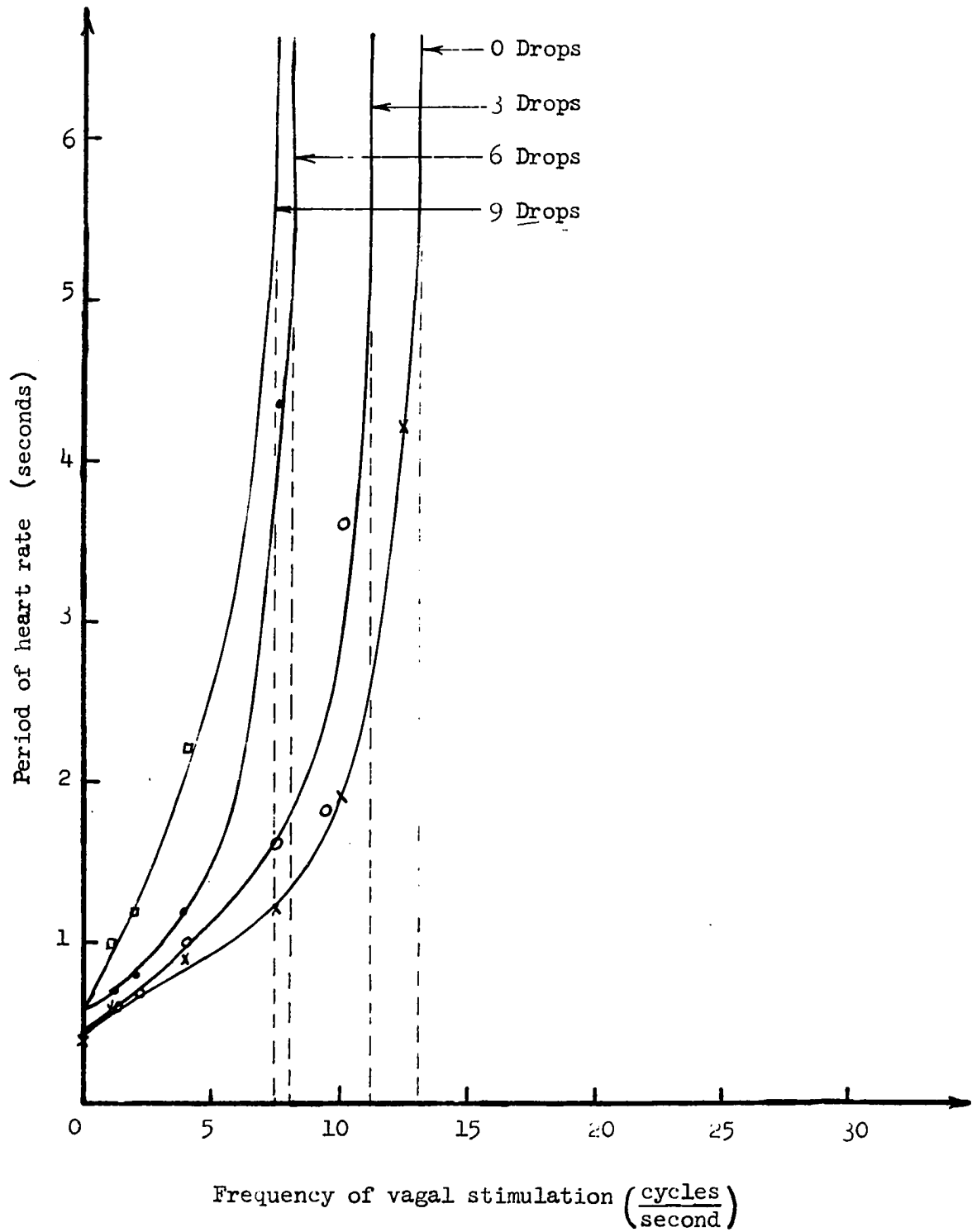


Figure 8. Period of heart rate vs. frequency of vagal stimulation (under the influence of varied amounts of physostigmine)

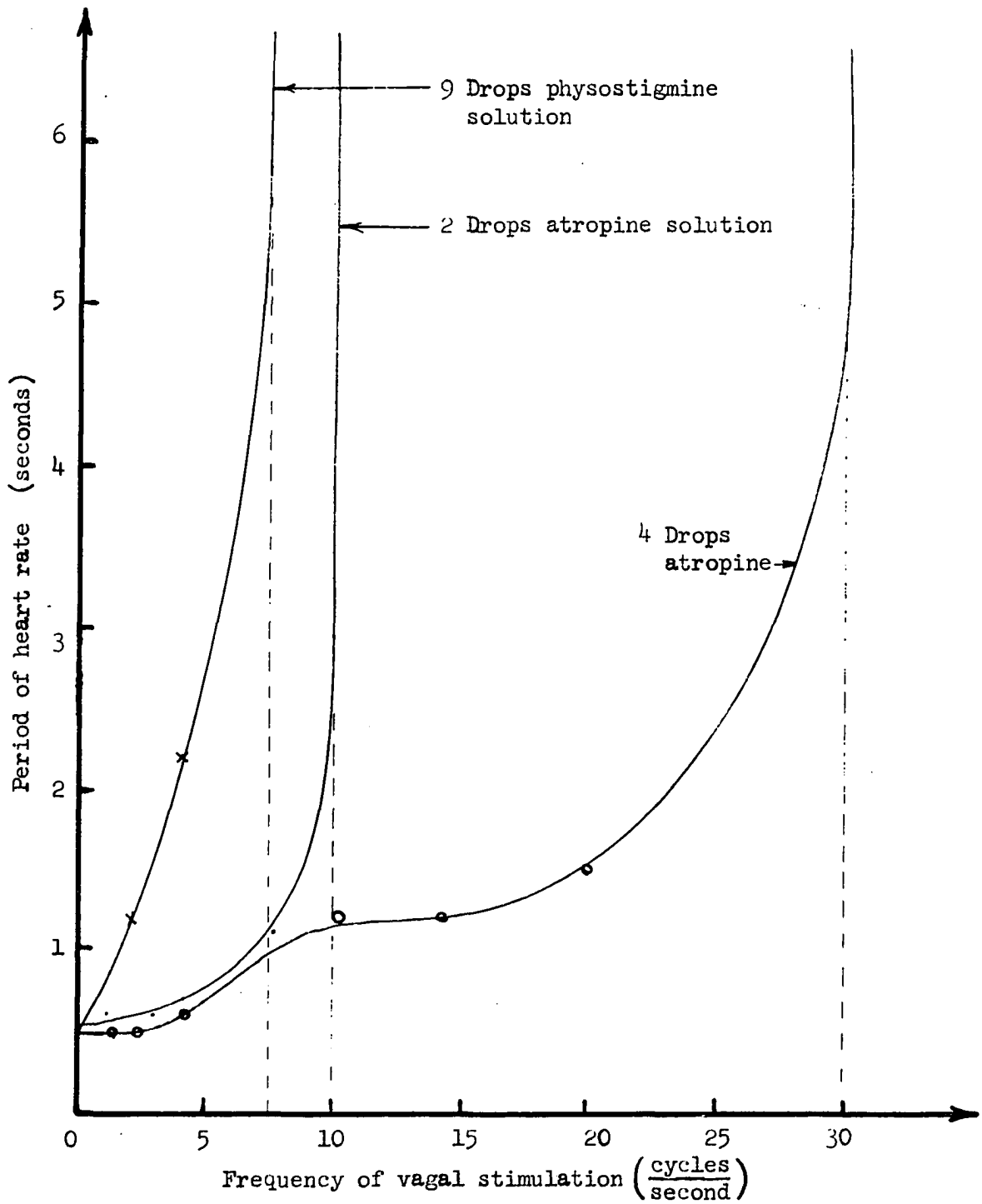


Figure 9. Period of heart rate vs. frequency of vagal stimulation (under the influence of varied amounts of atropine)

only a qualitative experiment, more work must be done to quantitatively prove or disprove the model or the development leading to the predictions made. This could possibly be done by using an isolated sinoatrial node preparation. With such a preparation, possibly in a modified Ringer's solution, the concentrations of physostigmine and atropine could be monitored along with the pacemaker rate and stimulation frequency (1). This would allow a quantitative study of their effects and thus a test for substantiating the validity of inequality 3.27 of Chapter III.

V. STATE VARIABLE MODEL FOR CAROTID SINUS HEART RATE REFLEX

A. Introduction

The previous chapters have dealt with the mathematical analysis of the sinoatrial node and vagal influence on this node. This chapter will expand the analysis to a larger system containing the carotid sinus pressoreceptors. It is believed that these bodies, located in the aorta and at the bifurcation of the internal and external carotids, are pressure sensitive. Bronk and Stella have experimentally illustrated variable frequency pulse trains emanating from the receptors at the carotid bifurcation (3). They have obtained data which related the frequency of impulses to the perfused carotid sinus pressure. These pulse trains travel along the carotid sinus nerve to the glossopharyngeal nerve. From this nerve, it is believed, the impulses travel to the vasomotor center in the reticular formation of the medulla, where they are processed before traveling down the vagus nerve to the sinoatrial node (26). It has also been found that these receptors not only regulate heart rate, but also have an effect on respiration. This point will be illustrated in the following chapter.

B. Mathematical Model

Using the results obtained by Bronk and Ferguson (2), Warner (37) postulated that the carotid sinus pressoreceptors produced impulses at a frequency dependent on both the static pressure of the region and the rate of change of that pressure with respect to time. Warner's mathematical description of this behavior is represented by the following equation:

$$f_1(t) = k_1 \frac{d(P(t) - P_0)}{dt} + k_2 (P(t) - P_0), \quad (5.1)$$

where $f_1(t)$ is the frequency of impulses on the carotid sinus nerve, k_1 and k_2 are constants to be determined, and $P(t)$ is the perfusion pressure. P_0 is a minimum pressure below which the pressoreceptors are insensitive to changes in pressure. This model has been modified by Grodins' (13, p. 181) to be of a form similar to

$$\tau \frac{df_1(t)}{dt} + f_1(t) = k_1 \frac{d[P(t) - P_0]}{dt} + k_2 [P(t) - P_0], \quad (5.2)$$

where τ is a time constant associated with the carotid sinus. This latter equation will be used in the following mathematical analysis. The last term on the right hand side of Equation 5.2 differs from Grodins model in that it is a linear approximation of the steady state ratio between pulse frequency and perfused carotid sinus pressure (3).

In this development, the influence of the brain on the impulses from the carotid sinus was postulated to be an attenuation of the pulse frequency as well as a noticeable time delay. The reasons for postulating this function were:

1. Since the normal frequency range of the impulse trains in the carotid sinus is from 50 to 140 impulses per second and the normal frequency range of the vagus impulse trains used in the previous chapter are roughly from 0 to 2 impulses per second, a

possible transfer function is an attenuation constant (35).

2. In data obtained in the experiments described later, a delay of 1 second between the impression of pressure on the carotid sinus and a noticeable heart rate change was noted consistently in all records. There are numerous points where this delay could occur. It could be contributed by the carotid sinus, the conduction of impulses along the nerves, the passage of impulses through the brain, or the sinoatrial node itself; however, all except the brain can be eliminated. The carotid sinus transfer function, from pressure to impulse frequency, has been shown by Bronk and Stella (3) to have a very small delay. This delay is much less than 1 second. The conduction velocity of the carotid sinus nerves has been found to be near 33 meters per second (25). Since the total path travelled from the sinus to the sinoatrial node is less than 1 meter, this is ruled out as a possible explanation of the delay. The response to vagal stimulation of the sinoatrial node in Warner and Cox's experiments shows no delay either, thus eliminating all areas except the brain. To further substantiate Warner and Cox's results, the same type of experiment was run on one dog. The experimental procedure is described in Chapter IV. Figures 10 and 11 show the results for two frequencies of stimulation. It is evident that there is little lag between vagal stimulation and the heart rate response.

Experiments were not run definitely to confirm the above postulate; however, the above reasoning and evidence discussed strongly suggests this conclusion.

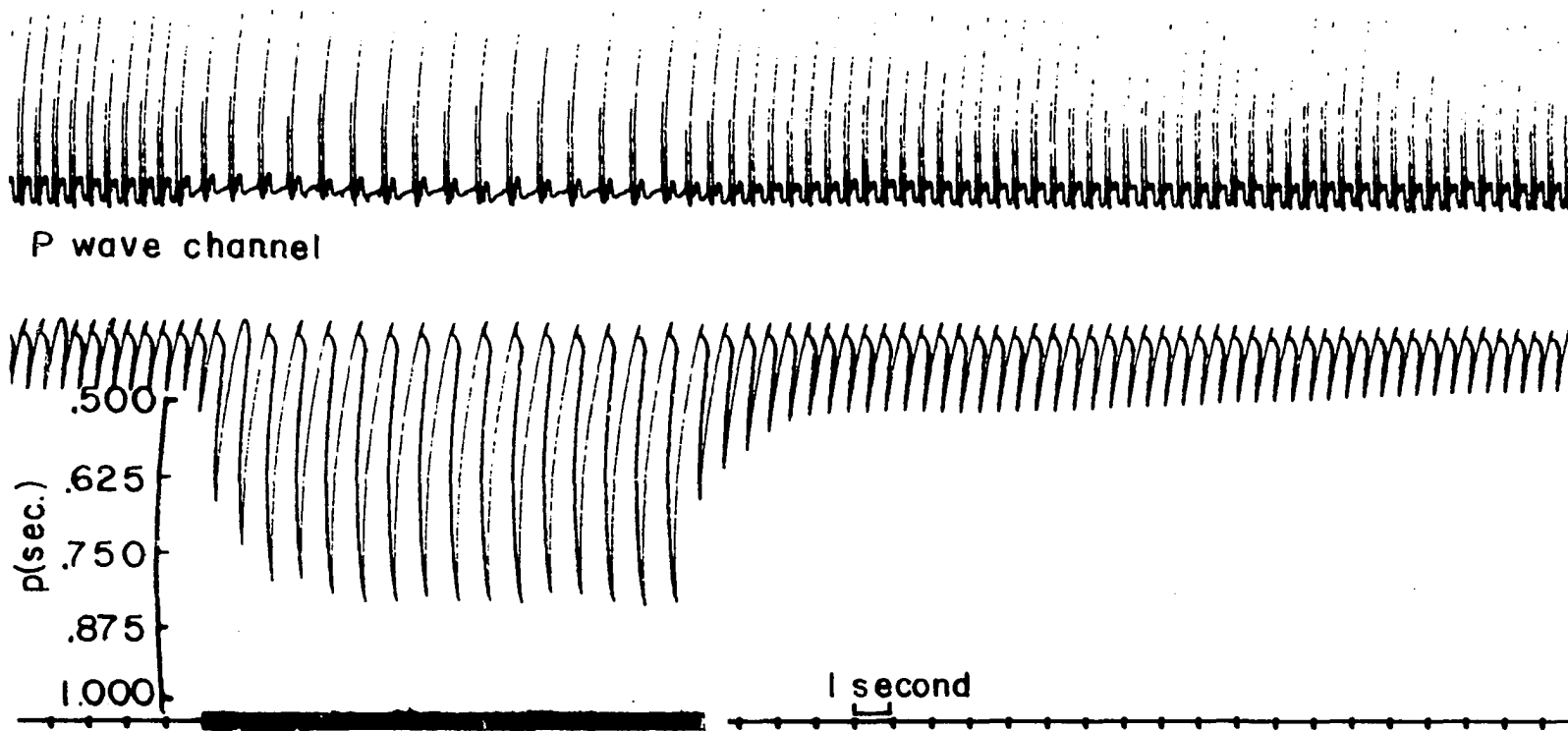


Figure 10. Period of the heart rate as a function of time during vagal stimulation (frequency of stimulation, 3 cycles per second, intensity, 30 volts)

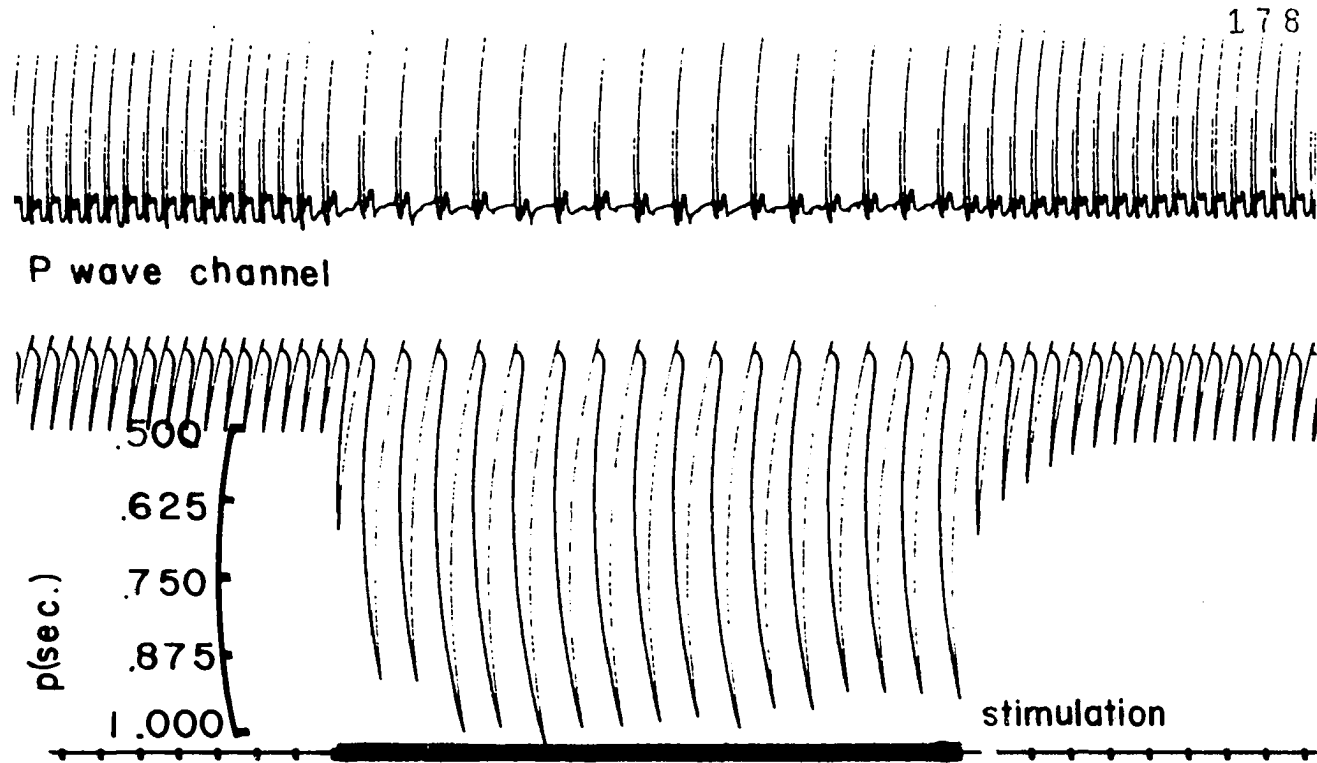


Figure 11. Period of the heart rate as a function of time during vagal stimulation (frequency of stimulation, 4 cycles per second, intensity, 30 volts, time markings at one second intervals)

The equations used previously for determination of the period of the sinoatrial node potential are again used in this development. The complete block diagram of the system studied is shown in Figure 12. The carotid sinus nerve impulse frequency is determined by Equation 1 and this is processed by an attenuation constant K_b in the brain. A delay of one second is introduced before the resulting impulse train travels down the vagus nerve to the sinoatrial node. At the sinoatrial node, the vagal frequency, f_2 , is used as a parameter in the state variable formulation describing the sinoatrial node potential.

Examination of the block diagram of Figure 12 reveals that the effect of carotid sinus stimulation by an increase of pressure at the site is a rise in vagal impulse frequency and this information (frequency of impulses on the vagus nerve) is used in the sinoatrial node equations as a parameter. The numerical problem of finding the time variation of heart rate period for specified pressure input at the carotid sinus is therefore the solution of the sinoatrial node equations with time varying coefficients determined by vagal impulse frequency f_2 and the iteration period Δt_n .

In matrix notation, the sinoatrial node system can be represented as follows:

$$\begin{bmatrix} \dot{N}(t) \\ \dot{C}_2(t) \end{bmatrix} = \begin{bmatrix} -(k_7 + k_8 f_2) & 0 \\ \frac{n f_8 f_2 C_1}{V_2} & -\frac{k_9}{V_2} \end{bmatrix} \begin{bmatrix} N(t) \\ C_2(t) \end{bmatrix} + \begin{bmatrix} k_7 N_m \\ 0 \end{bmatrix} u(t), \quad (5.3)$$

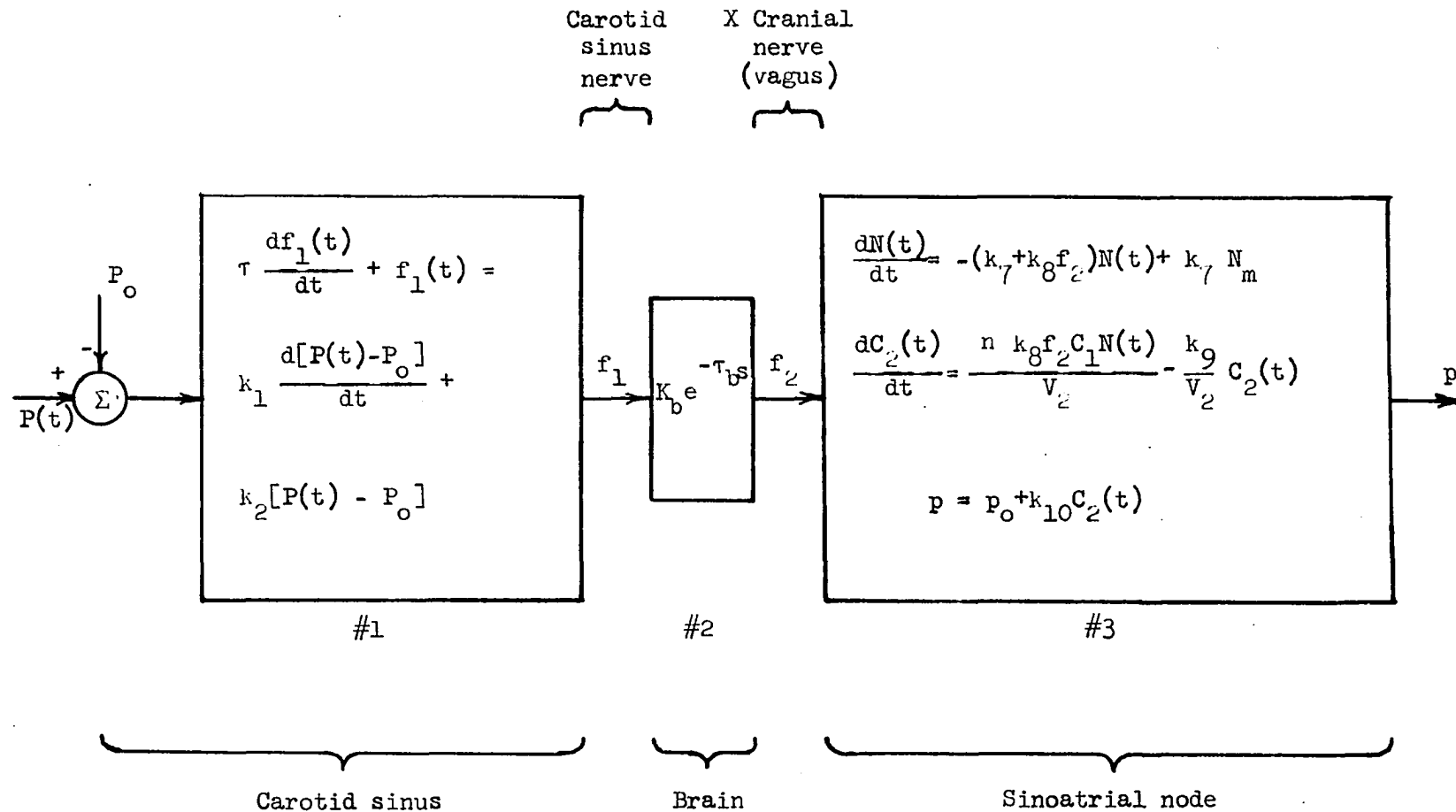


Figure 12. Block diagram representing each part of the carotid sinus heart rate reflex

where $u(t)$ represents a step function of unit amplitude from $t = 0$ to $t = \infty$. In order to compute the transition matrix $\phi(t)$ the matrix $[sI-A]$ of Chapter II must be evaluated. It is,

$$[sI-A] = \begin{bmatrix} s + (k_7 + k_8 f_2) & 0 \\ -\frac{nk_8 f_2 C_1}{V_2} & s + \frac{k_9}{V_2} \end{bmatrix}. \quad (5.4)$$

The inverse of this matrix is computed as,

$$[sI-A]^{-1} = \begin{bmatrix} \frac{1}{s + k_7 + k_8 f_2} & 0 \\ \frac{nk_8 f_2 C_1}{V_2 (s + k_7 + k_8 f_2) (s + \frac{k_9}{V_2})} & \frac{1}{(s + \frac{k_9}{V_2})} \end{bmatrix}. \quad (5.5)$$

From Equation 2.12 in Chapter II,

$$\phi(\Delta t) = \mathcal{L}^{-1} \left\{ [sI-A]^{-1} \right\} = \begin{bmatrix} e^{-(k_7 + k_8 f_2)\Delta t} & 0 \\ \frac{nk_8 f_2 C_1}{V_2 [k_7 + k_8 f_2 - \frac{k_9}{V_2}]} \left(e^{-\frac{k_9}{V_2} \Delta t} - e^{-(k_7 + k_8 f_2)\Delta t} \right) & e^{-\frac{k_9}{V_2} \Delta t} \end{bmatrix}. \quad (5.6)$$

The general solution of the system is then

$$\underline{X}(t_{n+1}) = \underline{\phi}(\Delta t_n) \underline{X}(t_n) + \int_{t_n}^{t_{n+1}} \underline{\phi}(t_{n+1}-\tau) \underline{B}u(\tau) d\tau. \quad (5.7)$$

Since in the problem being considered $\underline{\phi}(\Delta t_n)$ is constant throughout each iteration interval, $t_{n+1} - t_n = \Delta t_n$, it is convenient to change the limits of integration on the convolution integral to $\tau = 0$ and $\tau = \Delta t_n$. Thus,

$$\underline{X}(t_{n+1}) = \underline{\phi}(\Delta t_n) \underline{X}(t_n) + \int_0^{\Delta t_n} \underline{\phi}(\Delta t_n - \tau) \underline{B}u(\tau) d\tau. \quad (5.8)$$

Substituting the appropriate elements for $\underline{\phi}(\Delta t_n - \tau)$ and observing that

$$\underline{B} = \begin{bmatrix} k_7 N_m \\ 0 \end{bmatrix}, \quad (5.9)$$

the integral can be represented by the following matrix,

$$\int_0^{\Delta t_n} \underline{\phi}(\Delta t_n - \tau) \underline{B}u(\tau) d\tau = \begin{bmatrix} \int_0^{\Delta t_n} k_7 N_m e^{-(k_7 + k_8 f_2)(\Delta t_n - \tau)} d\tau \\ \int_0^{\Delta t_n} \frac{k_7 N_m (n C_1 k_8 f_2)}{V_2 (f_7 + k_8 f_2 - \frac{k_9}{V_2})} \left(e^{-\frac{k_9}{V_2}(\Delta t_n - \tau)} - e^{-(k_7 + k_8 f_2)(\Delta t_n - \tau)} \right) d\tau \end{bmatrix}. \quad (5.10)$$

Evaluating the integrals within the matrix,

$$\int_0^{\Delta t_n} \phi(\Delta t_n - \tau) \underline{B}u(\tau) d\tau$$

$$= \begin{bmatrix} \frac{k_7 N_m}{k_7 + k_8 f_2} (1 - e^{-(k_7 + k_8 f_2) \Delta t_n}) \\ \frac{k_7 N_m (n C_1 k_8 f_2)}{V_2 (k_7 + k_8 f_2 - \frac{k_9}{V_2})} \frac{V_2}{k_9} (1 - e^{-\frac{k_9}{V_2} \Delta t_n}) - \frac{1}{k_7 + k_8 f_2} (1 - e^{-(k_7 + k_8 f_2) \Delta t_n}) \end{bmatrix} \cdot$$

(5.11)

The entire matrix solution for the time variation of $N(t)$ and $C_2(t)$ is then:

$$\begin{bmatrix} N(t_{n+1}) \\ C_2(t_{n+1}) \end{bmatrix} = \begin{bmatrix} e^{-(k_7 + k_8 f_2) \Delta t_n} & 0 \\ \frac{n k_8 f_2 C_1}{V_2 (k_7 + k_8 f_2 - \frac{k_9}{V_2})} (e^{-\frac{k_9}{V_2} \Delta t_n} - e^{-(k_7 + k_8 f_2) \Delta t_n}) & e^{-\frac{k_9}{V_2} \Delta t_n} \end{bmatrix} \begin{bmatrix} N(t_n) \\ C_2(t_n) \end{bmatrix}$$

$$\left[\begin{array}{l} \frac{k_7 N_m}{k_7 + k_8 f_2} (1 - e^{-(k_7 + k_8 f_2) \Delta t_n}) \\ + \\ \frac{k_7 N_m (n C_1 k_8 f_2)}{V_2 (k_7 + k_8 f_2 - \frac{k_9}{V_2})} \frac{V_2}{k_9} (1 - e^{-\frac{k_9}{V_2} \Delta t_n}) - \frac{1}{k_7 + k_8 f_2} (1 - e^{-(k_7 + k_8 f_2) \Delta t_n}) \end{array} \right] . \quad (5.12)$$

Matrix Equation 5.11 translates the states $N(t_n)$ and $C_2(t_n)$ to $N(t_{n+1})$ and $C_2(t_{n+1})$. This development is dependent on the fact that all the elements in the matrices involved are constant within each iteration interval. In order to compare the results of this formulation with experimental evidence, it is necessary to obtain numerical values for the constants in the equations. Values for some constants can be found in Warner and Cox's article (38);

$$k_7 = 2.75 \frac{1}{\text{second}} ,$$

$$k_8 = 0.69 \frac{1}{\text{action potential}} ,$$

$$k_9 = 0.87 \frac{1}{\text{second}} ,$$

and

$$V_2 = \text{unit volume} .$$

From a comparison of the equation describing the steady state concentration of $C_2(t = \infty)$ in Appendix A and the equation for period shown in Warner and Cox's Figure 10 of their paper (38), the following relation is obtained,

$$n C_1 = \frac{0.65 k_9}{k_8 k_{10} N_m} .$$

The constants f_2 and Δt_n are yet to be determined. The constant Δt_n is chosen to be 1 second in order to reduce computations since they were done by hand and not computer. This interval is equal to or smaller than the intervals over which any matrix element changes value in the matrix equation during the time solution, therefore, it does not affect the accuracy of the final solution.

A piecewise constant function, $f_2(t)$, is obtained from Equation 5.2 through an averaging process explained in Appendix C. The constants k_1 , k_2 , and τ are adjusted by trial and error to give the best fit between theoretical and experimental results.

Substituting the above values for k_7 , k_8 , k_9 , V_2 and $n C_1$ into Equation 5.12,

$$\begin{bmatrix} N(t_{n+1}) \\ C_2(t_{n+1}) \end{bmatrix} = \begin{bmatrix} e^{-(2.75 + 0.69 f_2)\Delta t_n} & 0 \\ \frac{0.565 f_2 (e^{-0.87\Delta t_n} - e^{-(2.75+0.69f_2)\Delta t_n})}{k_{10} N_m (1.88+0.69 f_2)} & e^{-0.87\Delta t_n} \end{bmatrix} \begin{bmatrix} N(t_n) \\ C_2(t_n) \end{bmatrix}$$

$$\begin{aligned}
 & + \left[\frac{2.75N_m}{2.75+0.69f_2} e^{-(2.75+0.69f_2)\Delta t_n} \right. \\
 & \left. \frac{1.55f_2}{k_{10}(1.88+0.69f_2)} \left[1.15(1-e^{-0.87\Delta t_n}) - \frac{(1-e^{-(2.75+0.69f_2)\Delta t_n})}{2.75+0.69f_2} \right] \right] \quad (5.13)
 \end{aligned}$$

With Δt_n equal to 1 second and f_2 determined by the method in Appendix C, a value for $C_2(t_{n+1})$ is found. Then the equation for heart rate is,

$$p(t_{n+1}) = p_o + k_{10} C_2(t_{n+1}) \quad (5.14)$$

where $p_o = 0.5$ seconds, thus

$$p(t_{n+1}) = 0.5 + k_{10} C_2(t_{n+1}). \quad (5.15)$$

With these equations and a step input of pressure of 300 mm. Hg, or

$$P(t) = 300 u(t), \quad (5.17)$$

the theoretical variation in period is calculated in Appendix C. The resulting theoretical curve for the period variation is shown in Figure 13.

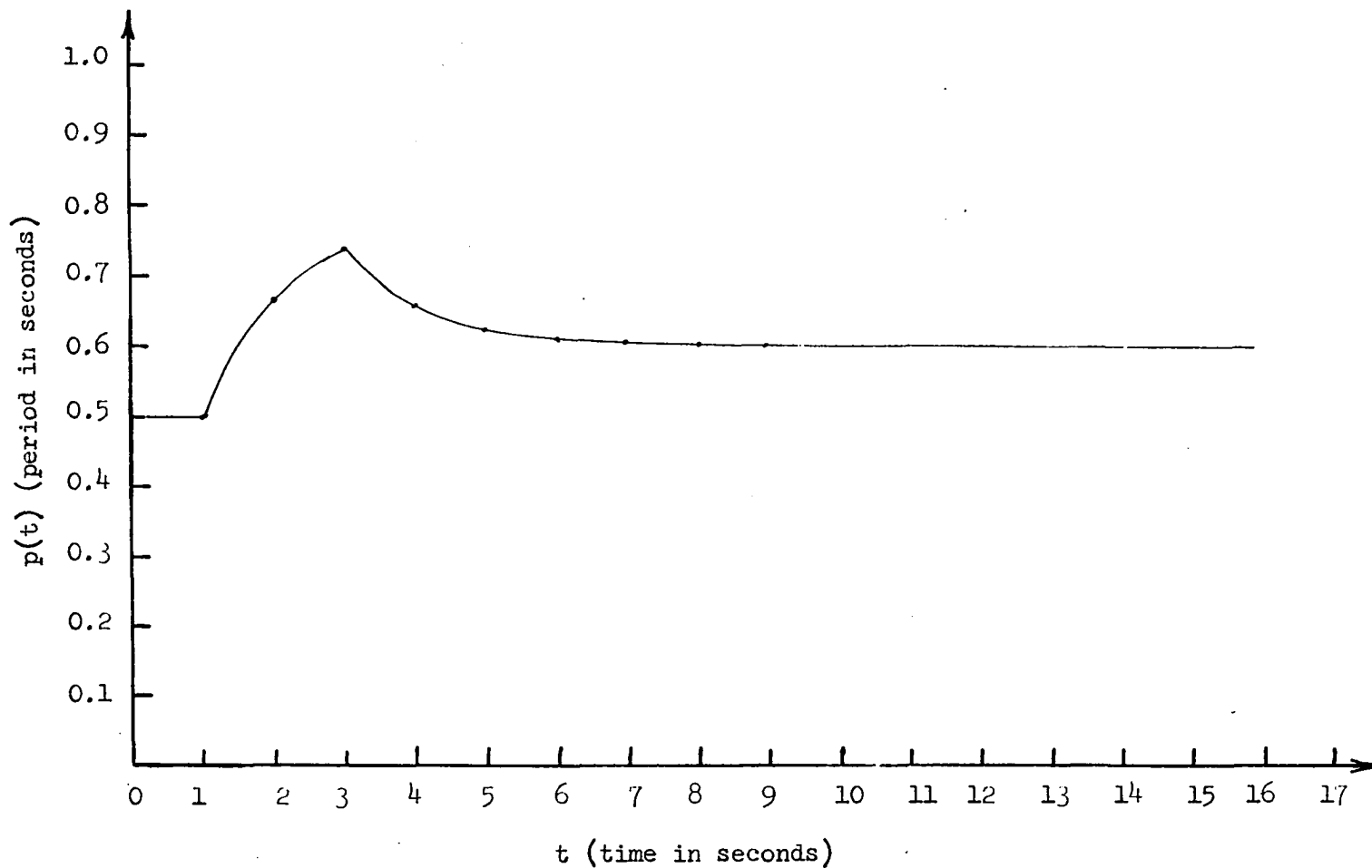


Figure 13. Theoretical curve for heart rate reflex for a step input of pressure at the carotid sinuses (300 mm. Hg step applied at $t = 0$)

VI. EXPERIMENTAL RESULTS FOR CAROTID SINUS HEART RATE REFLEX

A. Experimental Procedure

The purpose of the experiment was to record the response of the period of heart rate when the carotid sinus pressoreceptors were stimulated by a specified perfusion pressure. The pressure used during this experiment was a step of magnitude equal to 300 mm. Hg.

The experiment was run on five mongrel dogs, both male and female, weighing 15 to 30 pounds. Three different procedures were used to anesthetize the dogs and they are listed below:

Procedure #1. Initially, intravenous injection of 30 mgm/kg of sodium pentobarbital and supplemented as needed.

Procedure #2. Initially, intravenous injection of 110 mgm/kg of α -chloralose and supplemented as needed.

Procedure #3. Initially intravenous injection of 10 mgm/kg of thiopental sodium, and supplemented as needed, plus 30 mgm/kg of α -chloralose.

The α -chloralose solution was injected while warm (65° - 70° Centigrade) because of its low solubility in water. It was prepared as a 1% solution in 1 liter lots by heating at 80° Centigrade for 8-10 hours. In all preparations the sympathetic nervous activity was blocked by the administration of 0.5 mgm/kg dihydroergotamine intravenously (36).

Isolation of the left and right carotid sinus was accomplished by two incisions, one to the left and one to the right of the midline of the neck and directly above the separation of the sternocephalicus and sternohyoideus muscles, beginning at the level of the cricoid cartilage, or slightly below, and ending near the base of the mandible. On each side,

the sternocephalicus and sternohyoideus muscles were separated and the thyroid gland retracted laterally to expose the common carotid bifurcation into internal and external branches. The internal carotid, occipital, external carotid and lingual arteries, which were distinguishable from nervous and fatty tissue, were ligated. Care was taken to preserve the carotid sinus nerve which emerged on the medial side of the bifurcation of the common carotid artery and proceeded cranial alongside the internal carotid artery.

Figure 14 shows schematically how the experiment was set up for applying a pressure function to both left and right carotid sinuses simultaneously. The measured variables were period of the heart rate, perfusion pressure, and respiration. The pressure was applied to the carotid sinuses by cannulating both common carotids 2 to 3 inches caudad to the bifurcation and inserting Horsley needles into the arteries. Heparinized saline was used for the perfusion solution.

While clamping the pressure line to the carotids, the pressure regulator could be set to give a step of 300 mm. Hg when the 3-way valve was set in the position to pressurize the pressure bottle. With the regulator set to a pressure of 300 mm. Hg and the 3-way valve turned to the position which opened the pressure system to the outside air, the clamp was removed. When the step of 300 mm. Hg pressure was desired, the 3-way valve was turned to connect the regulator to the system, thus impressing a pressure, via the saline, onto each carotid sinus. The pressure was removed by rotating the 3-way valve to allow continuity with room air. This system was used in order to maintain a steady pressure. It was very difficult to ligate all of the small arteries which emanate from the

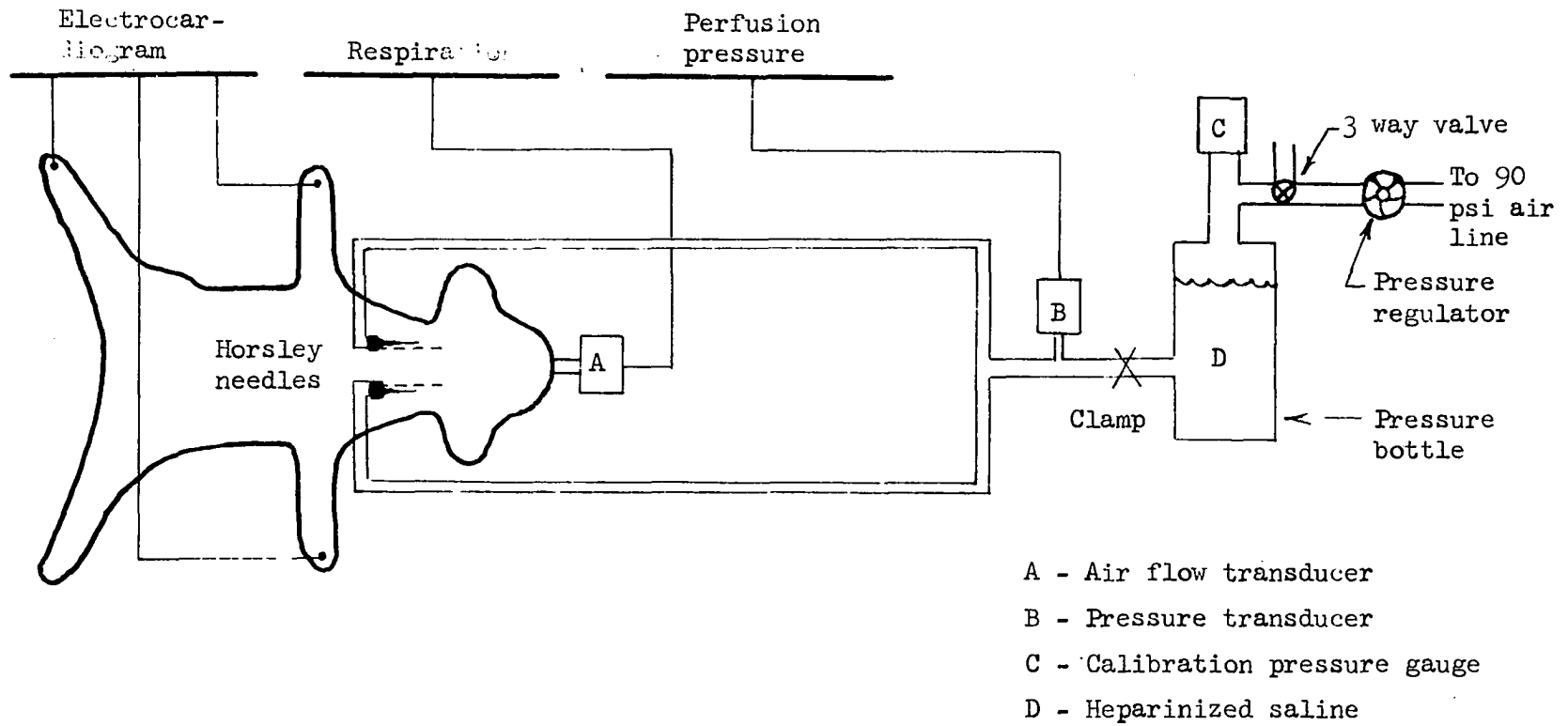


Figure 14. Diagram of experimental procedure for carotid sinus pressure perfusion

carotid sinus area and therefore there was a small amount of leakage. The capacity of the air line was sufficient to keep a steady pressure on the carotid sinus preparation even though there was a slow, but constant, loss of fluid through the untied arteries. Heymanns and Bouckaert (15) and also Chungcharoen, et al. (6) have written excellent descriptions of the carotid sinus area. Figure 15a and 15b are included here to show the fine anatomical features of the arterial supply to the area. Figure 15a shows a latex rubber cast taken from a canine cadaver the arterial system of which had been injected. It is interesting to note, in this preparation, the very fine communicating branch between the left occipital and internal carotid arteries. This serves to point out the difficulties involved when an attempt is made to completely isolate and pressurize the carotid sinus area.

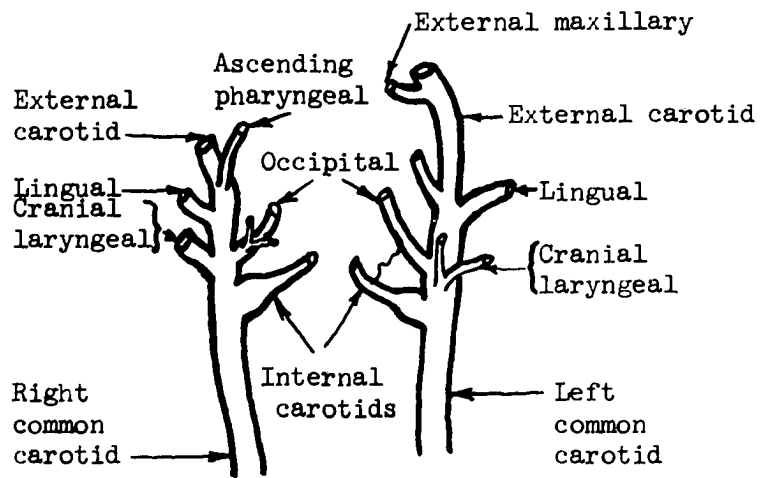
The data obtained was recorded by the Grass Model 5 Polygraph. Three channels of its six channel capacity were used. Respiration was monitored by measuring the pressure differential across a fine wire mesh which was caused by a flow of air through the mesh. The animals breath was the actual air flow measured and the differential pressure was measured with a Grass volumetric pressure transducer, PT 5A. The perfusion pressure was measured with a Grass physiological transducer, P23AC (capable of measuring pressures from 0 to 750 mm. Hg).

B. Discussion of Experimental Results

Figures 16, 17, 18, and 19 show the response of the heart rate period, p , as a function of time for a pressure input of 300 mm. Hg on the carotid sinus receptors. Dog A, used in Figures 16, 17, and 18, was a 30



(a) Photograph of carotid artery casts



(b) Diagram of carotid arteries

Figure 15. Anatomical features of the carotid arteries near the carotid sinuses (24, p. 288)

pound male and Procedure #1 was used for administration of the anesthetic. Dog B, used in Figure 19, was a 25 pound male and Procedure #3 was used for administration of the anesthetic. The most evident observation is that the response is not consistent, but varies in maximum amplitude and possibly shape. This variation may be caused by fatigue of the carotid sinus receptors due to prolonged stimulation (3). The responses of Figures 16 and 17 were taken from a series of stimulations separated by 30 to 40 second rest intervals, while Figure 18 was taken after the preparation was allowed to rest for at least 3 minutes. There is a noticeably larger response in Figure 18. A longer portion of the record was included in Figure 18 to show the slow return of the period to normal.

Another possible reason for this inconsistency may be explained by considering the impulse frequency on the vagus nerve. Since at zero pressure the vagal impulse frequency due to carotid sinus innervation is very low, possibly 1 impulse every 20 seconds, it is important to know at what instant between pulses the stimulation occurs. If it is sufficiently close to the last pulse generated in the pulse train corresponding to zero pressure, it would then create a much higher frequency of innervation than if the stimulation was in the middle or close to the end of the zero pressure pulse interval. This higher frequency of innervation would increase the initial acetylcholine concentration and thus raise the period of heart rate and thus affect the response curve.

On all Figures (16, 17, 18, and 19) of this section, a delay of approximately 1 second is evident between the onset of stimulation and the initial response by the heart rate period. It is interesting to note that this delay is not evident at termination of the stimulation. This seems

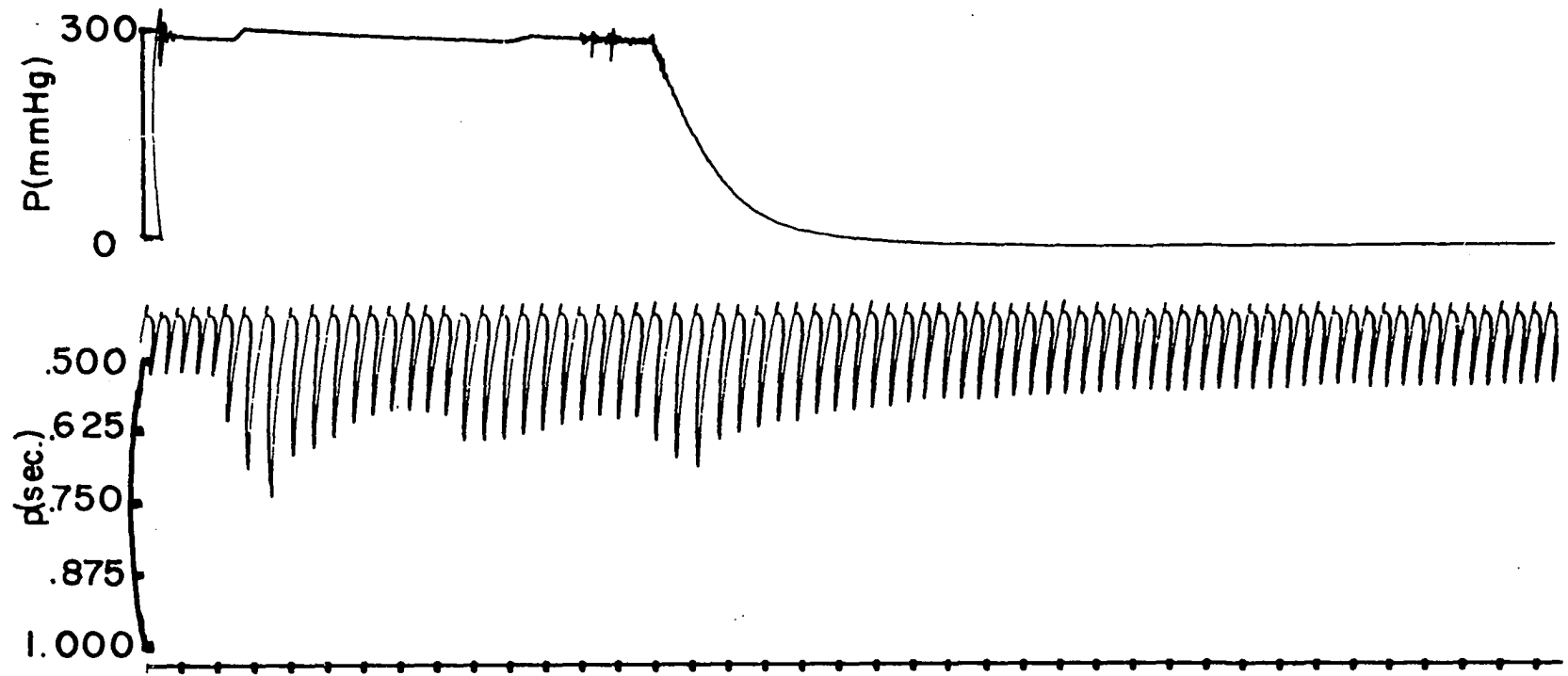


Figure 16. Experimental heart rate response for a step input of 300 mm. Hg pressure on the carotid sinuses

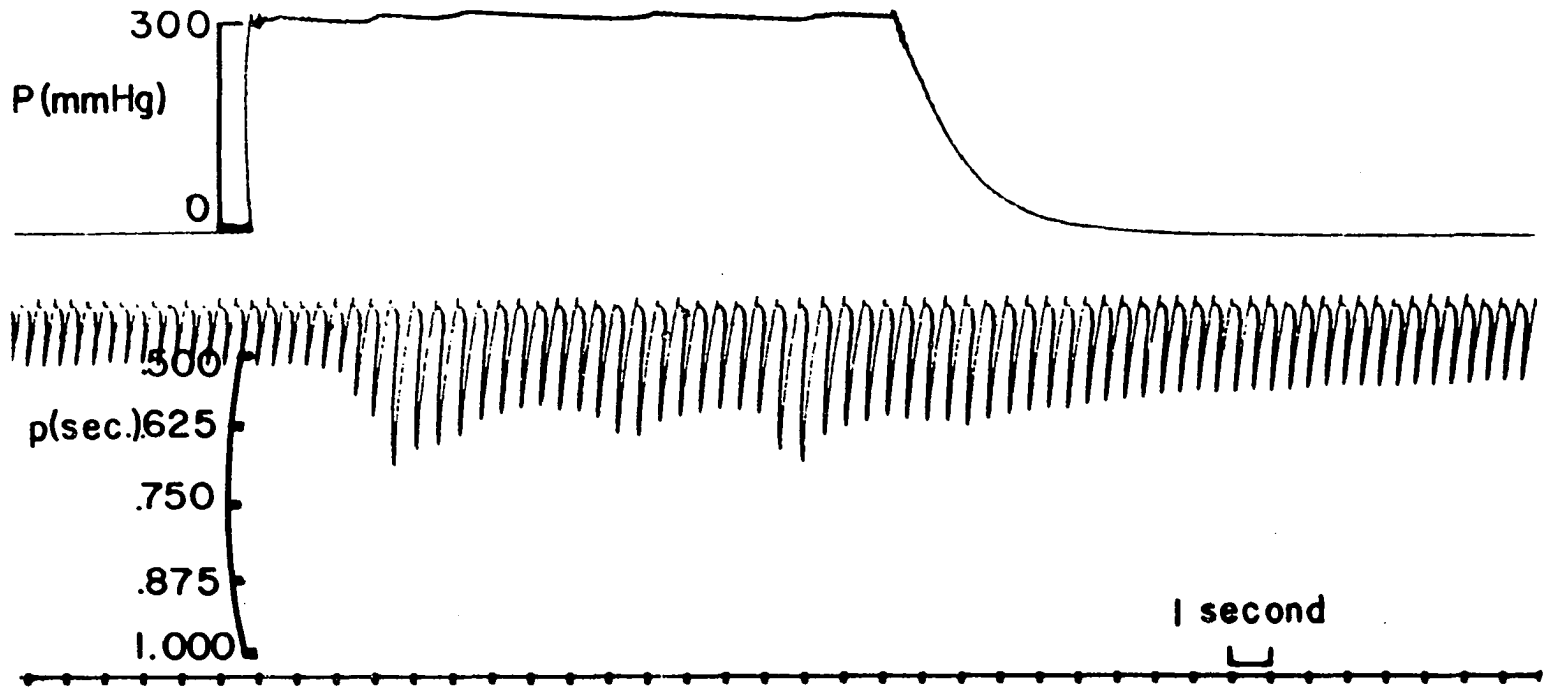


Figure 17. Experimental heart rate response for a step input of 300 mm. Hg pressure on the carotid sinuses

Figure 18. Experimental heart rate response for a step input of 300 mm. Hg pressure on the carotid sinuses

768

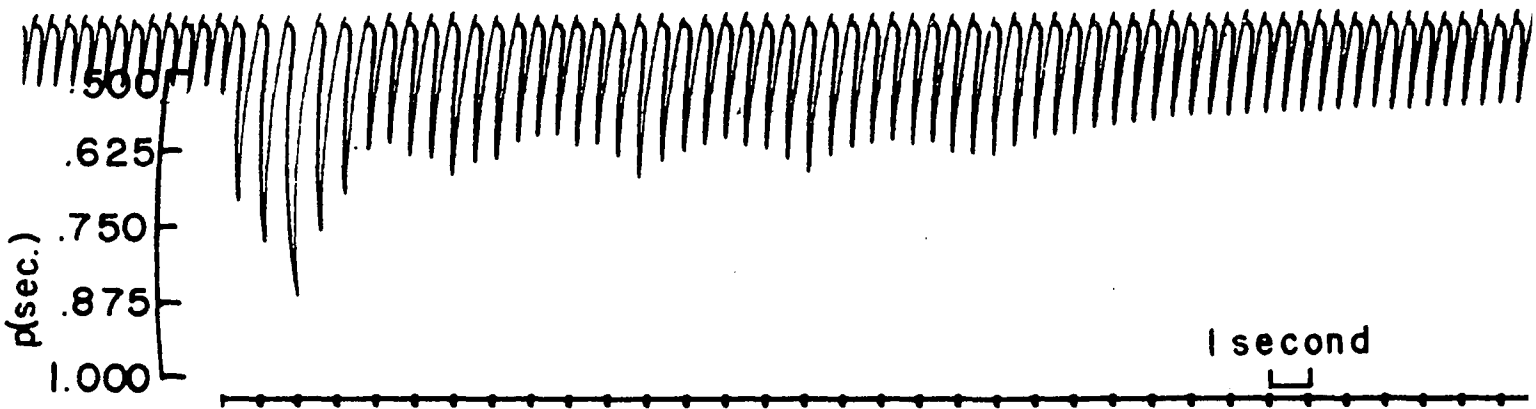
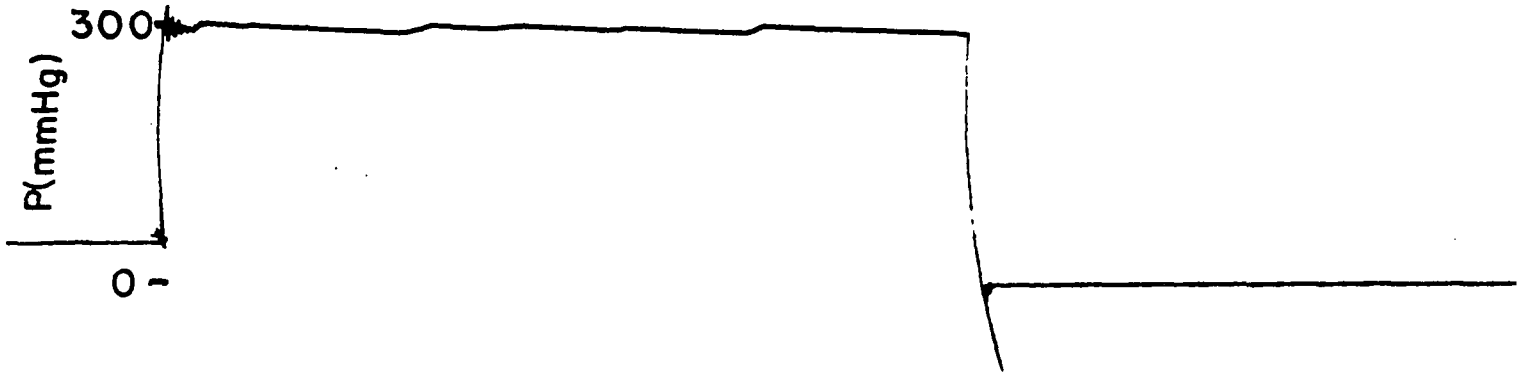
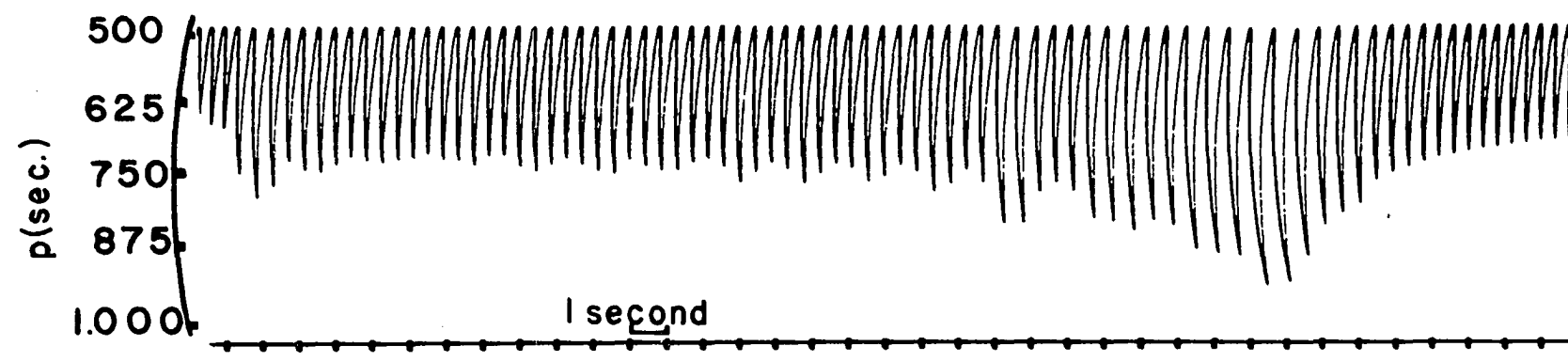
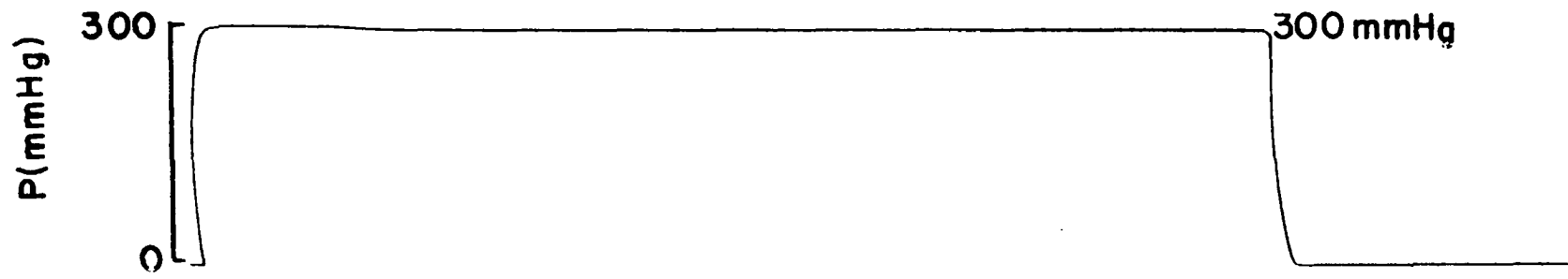
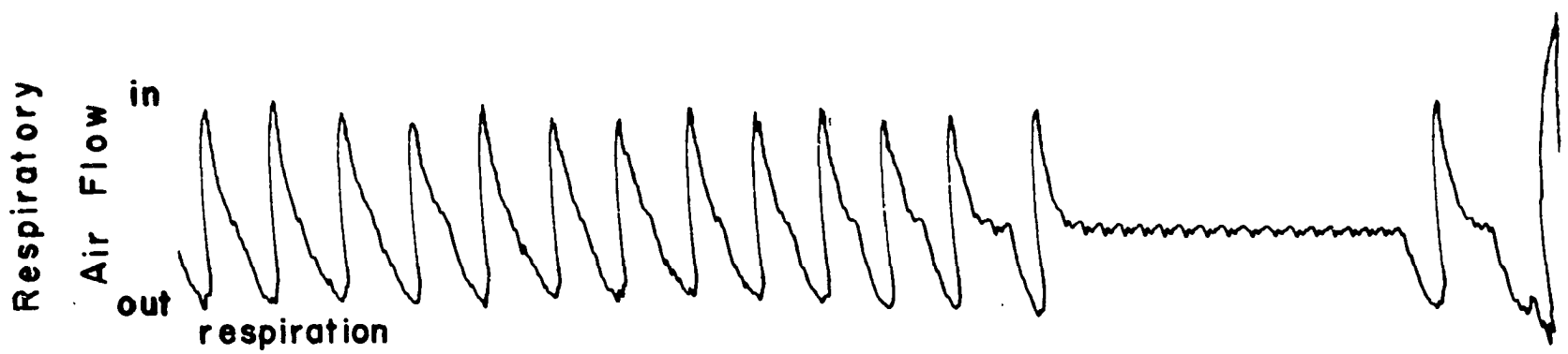




Figure 19. Carotid sinus pressure effect on respiration. The top channel is respiration with inspiration plotted. The second channel is carotid sinus perfusion pressure $P(t)$. The third channel is heart rate period, p , plotted downward



to support M. Clynes' theory of unidirectional rate sensitivity (8). Since this may be true, this report is interested in only the reflex due to the sudden increase and maintenance of pressure at the carotid sinus.

After the initial response there is a slow variation in heart rate which has a period of about 2 to 4 seconds. Figure 19 shows that this variation is synchronous with respiration. Therefore, this variation was attributed to respiration influence on heart rate.

Figure 20 shows a comparison of the curves resulting from experimental and calculated responses to a step input of 300 mm. Hg pressure on the carotid sinus. Table 1 is a compilation of theoretical results from Appendix C and experimental results from Figure 16. The calculated curve was fitted by varying the unknown constants k_1 , k_2 , and τ of Equation 5.2 in Chapter V. It should be noted that the shape of the curves agree quite well and that by choosing the proper constants it was possible to construct the calculated curve to within roughly a 10% error in magnitude at all points.

Table 1. Compilation of theoretical and experimental results for the heart rate period

t(seconds)	Theoretical p(t)	t(seconds)	Experimental p(t)
0	0.500	0	0.500
1.0	0.500	1.0	0.500
2.0	0.670	1.8	0.625
3.0	0.735	2.3	0.687
4.0	0.656	3.0	0.750
5.0	0.624	4.0	0.650
6.0	0.611	5.0	0.625
7.0	0.607	6.0	0.610
8.0	0.604	7.0	0.600
9.0	0.602	8.0	0.600

An interesting respiratory reaction to the pressure stimulation of the carotid sinus is shown on the top recording of Figure 19. It is evident that after a period of 25 to 30 seconds of pressure stimulation, respiration ceases until shortly after termination of the stimulus. This phenomenon was also reported by Heymanns and Bouckaert in their work on the dog (16). In their laboratory they tested for respiratory apnea both before and after denervation of the carotid sinus. They found no reaction after denervation and thereby concluded that this was a reflex reaction. In 1932, Carl F. Schmidt wrote an excellent review of the literature on this topic and did further research with rabbits, dogs, and cats (31,32). His conclusions were that the respiratory center in the brain was noticeably affected by its blood supply, and specifically by occlusion of the vertebral and carotid arteries. He also substantiated Heymanns and Bouckaert's previous work. His final evaluation of the phenomena of respiratory apnea was that it was due to a reflex, alterations in central blood flow to the respiratory center, or to both in combination. These conclusions leave much to be desired as far as the actual knowledge of carotid sinus influence on respiration is concerned, but are invaluable for a broad evaluation of the complete respiratory control mechanism.

At this point it is well to mention that during this particular experiment abnormal factors may be influencing the results. Dog A, used in Figures 16, 17, 18, was anesthetized with sodium pentobarbital as in Procedure #1 on page 52. Dog B, used in Figure 19, was anesthetized according to Procedure #3 on page 52. The latter procedure uses α -chloralose as the general anesthetic. It is well documented (4,9) that α -chloralose enhances the carotid sinus reflex mechanism concerned with heart rate.

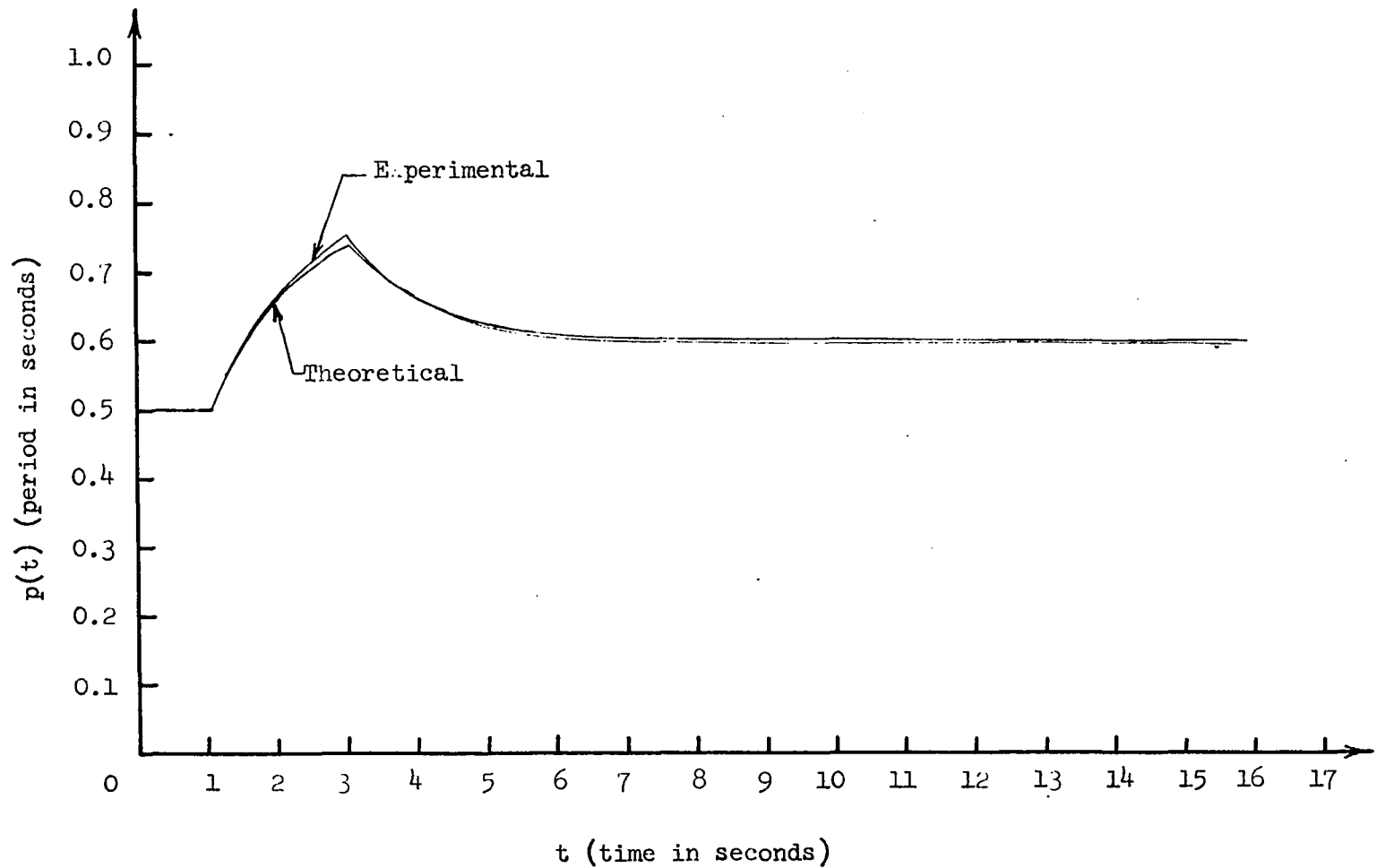


Figure 20. Comparison of theoretical and experimental results (experimental values taken from Figure 16, theoretical values calculated in Appendix C)

The above facts point out that the experimental procedures of these experiments are not satisfactory in the determination of the normal operations carried on within the central nervous system. This suggests further study in methods of implantable pressure sources and transducers in order to run the same experiments while the animal is conscious and not under the influence of anesthetics.

VII. THE USE OF STATE VARIABLES TO DESCRIBE A CLOSED LOOP FEEDBACK SYSTEM

A. Introduction

In the previous chapters an open loop analysis of the sinoatrial node and carotid sinus has been presented. This chapter will show how the entire heart rate feedback system, using the carotid sinus as the error detecting device, can be described using the methods of state variables. This analysis will use the previous results presented for those parts of the system which have been analyzed. Parts which have not been analyzed and which need further study will be indicated by a function notation. One other assumption, the form of the equation describing pacemaker potentials, will be discussed briefly but not rigorously developed from the intrinsic properties of the pacemaker.

B. Analysis

In block diagram form the system to be simulated is shown in Figure 21. The pressure produced by the heart ventricle mechanism is compared to a static pressure P_0 and this difference is converted to a frequency $f_1(t)$ on the carotid sinus nerve. In the brain, $f_1(t)$ is altered by a multiplication constant K_b and a time lag of τ_b seconds to produce $f_2(t)$, the vagal stimulation frequency. The vagal frequency is used in the previously discussed sinoatrial node equations to obtain the concentration of acetylcholine at the node $C_2(t)$.

The pacemaker potential equation

$$\frac{d^2 y}{dt^2} + \frac{4\pi^2}{(p_0 + k_{10} C_2(t))^2} y = 0 \quad (7.1)$$

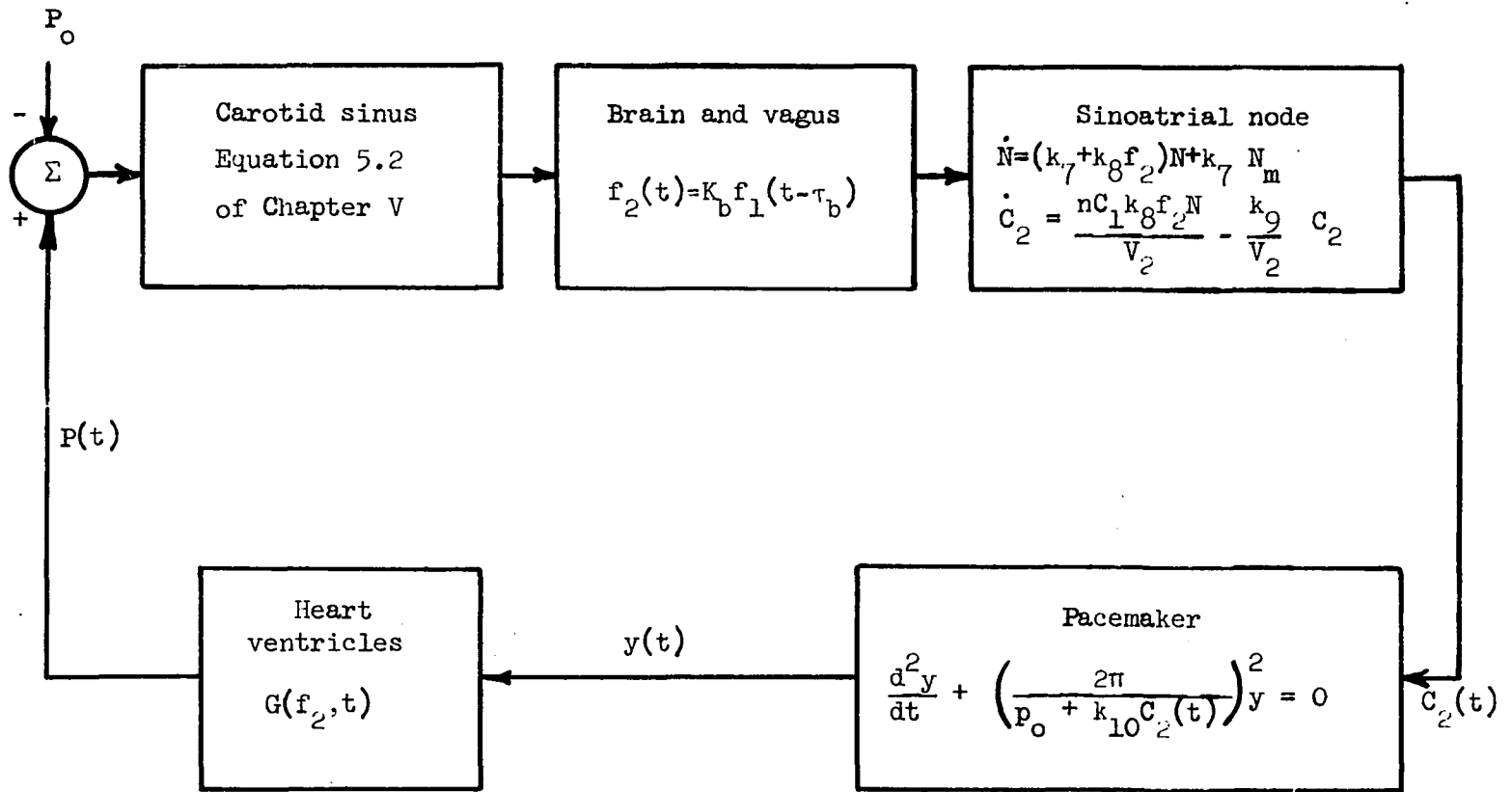


Figure 21. Block diagram of closed loop feedback system simulating carotid sinus heart rate control

is very similar to that proposed by Clynes (5), which is

$$\frac{d^2 y}{dt^2} + [4\pi^2 r_o^2 - V(t)]y = 0,$$

where $V(t) = f_2(t)$, the vagal stimulation frequency, and $r_o =$ the normal heart rate. For very small variations in $f_2(t)$, which correspond to small variations in $V(t)$, the variations of $C_2(t)$ will also be small, therefore,

$$\frac{4\pi^2}{[p_o + k_{10}C_2(t)]^2} \approx \frac{1}{p_o^2} \quad \frac{4\pi^2}{(1 + \frac{2k_{10}C_2(t)}{p_o})} \approx \frac{4\pi^2}{p_o^2} \left(1 - \frac{2k_{10}C_2(t)}{p_o}\right). \quad (7.2)$$

Thus, Equation 7.1 does agree in form with Clynes equation for small variations in vagal frequency if for these small concentrations $C_2(t)$ is proportional to $f_2(t)$. Since Equation 7.1 has been postulated only from evidence suggesting an oscillatory phenomena (30, p. 594), this area of the development needs more research, both theoretical and experimental, with the objectives of first establishing a rigorous development of the equation from physical properties of the pacemaker tissue and then experimentally testing the derived equation.

Another area for further research is in the effect of nervous innervation, both sympathetic and parasympathetic, of the ventricular muscle of the heart. In Figure 22 the transfer from the pacemaker potential $y(t)$ to pressure $P(t)$ is described by a function $G(f_2, t)$. It has been shown that the pressure is dependent on many factors within the muscle itself and that these factors are functions of numerous nervous innervations. Since this discussion is mainly interested in the influence of

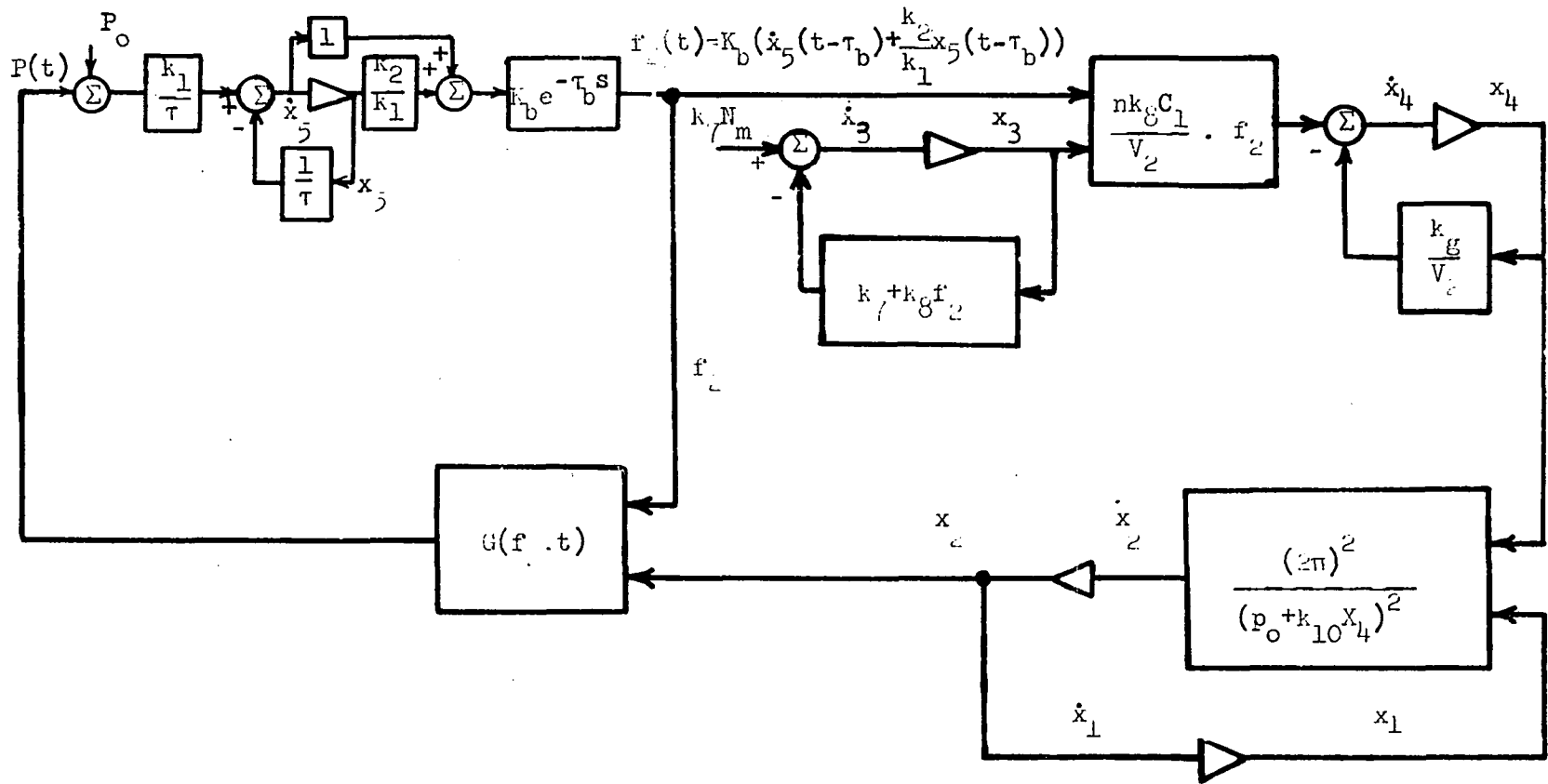


Figure 22. Analog computer diagram for heart rate feedback control

vagal stimulation, the function $G(f_2, t)$ will be assumed dependent only on time and the variable f_2 .

An analog diagram of the system can be represented as shown in Figure 22. From this diagram the state variable equations can be written as

$$\dot{x}_1 = x_2$$

$$\dot{x}_2 = \frac{(2\pi)^2}{(p_0 + k_{10}x_4)^2} x_1$$

$$\dot{x}_3 = -(k_7 + k_8 f_2) x_3 + k_7 N_m$$

$$\dot{x}_4 = \frac{nk_8 C_1 f_2 x_3}{V_2} - \frac{k_9}{V_2} x_4$$

$$\dot{x}_5 = [x_2 G(f_2, t) - P_0] \frac{k_1}{\tau} - \frac{1}{\tau} x_5$$

In matrix form, considering f_2 and x_4 slowly varying functions in relation to the iteration interval and therefore considering them constant during each interval,

$$\begin{bmatrix} \dot{x}_1 \\ \dot{x}_2 \\ \dot{x}_3 \\ \dot{x}_4 \\ \dot{x}_5 \end{bmatrix} = \begin{bmatrix} 0 & 1 & 0 & 0 & 0 \\ \left[\frac{2\pi}{p_0 + k_{10}x_4} \right]^2 & 0 & 0 & 0 & 0 \\ 0 & 0 & -(k_7 + k_8 f_2) & 0 & 0 \\ 0 & 0 & \frac{nk_8 C_1 f_2}{V_2} & -\frac{k_9}{V_2} & 0 \\ 0 & \frac{k_1 G(f_2, t)}{\tau} & 0 & 0 & -\frac{1}{\tau} \end{bmatrix} \begin{bmatrix} x_1 \\ x_2 \\ x_3 \\ x_4 \\ x_5 \end{bmatrix} + \begin{bmatrix} 0 \\ 0 \\ k_7 N_m \\ 0 \\ -\frac{k_1 P_0}{\tau} \end{bmatrix} .$$

(7.3)

The $\phi(\Delta t_n)$ matrix can be computed as a sum of a series (11). This can be done by a digital computer. Since matrix equation 4 implies a matrix for $\phi(\Delta t_n)$ order is 5 x 5, a computer solution may be the best answer when considering the hand labor involved to compute the required constants. The disadvantage of this scheme is the amount of time required to compute $\phi(\Delta t_n)$ before each iteration or transition. If this is necessarily long due to accuracy and convergence considerations, the entire problem solution may become excessively time consuming even on a digital computer.

VIII. CONCLUSION

The preceding chapters have been concerned with applying the state variable formulation to a specific biological control system. The purpose of this study was to point out the advantages and disadvantages of such a method of analysis in biological systems.

The analysis of stability using Liapunov's Second Method is a convenient tool in that it allows the inclusion of nonlinear terms in the development of conditions for stability. As of yet, however, the method of determining the Liapunov function has not been rigorously determined for all types of problems. Hopefully, more research in the method of finding the Liapunov function will disclose a method.

The development of the heart rate response curve for a step input of pressure at the carotid sinuses points out two advantages of the state variable formulation. First, as illustrated in Appendix A, the transfer functions may be changed at any time in the development of a solution. Second, as illustrated in Appendix C, the iteration rate can be varied and the matrix varied to insert information, in a stepwise fashion, into the system solution. These advantages seem to be useful in the specific type of problems dealing with pulse frequency modulation information and/or transfer functions whose form are dependent on the input signal. Since many biological systems have either one or both of these characteristics, the method is certainly a helpful tool in the analysis of such control systems.

The obvious disadvantages, which have been pointed out previously are the need for a digital computer to solve even the fairly simple problems and consequently the difficulty in externally changing parameters in

a simulation experiment. This may suggest an area of research in interface design to establish communication from easily varied external controls to the system matrix equations which are being operated upon by the digital computer.

Parts of this work have pointed out problems which need further expansion and experimental investigation. The following paragraphs explain briefly some other problems.

In the analysis of the carotid sinus heart rate reflex, the magnitudes of the impulses on nerve fibers were considered constant. Yet, many of the records in the literature do show a slight variation in amplitude and variations in stimulus intensity are very important when working with nerve conduction and innervation. It may be interesting to investigate what effects this intensity produces and possibly develop an amplitude noise analysis of certain body systems.

The curve suggested for acetylcholine destruction in Chapter III has not been verified experimentally. The reaction may be caused by and influenced by many factors which are not known. The assumption of a pure enzyme reaction has been used here, but there is evidence suggesting that diffusion also influences the reaction (38).

The pacemaker potential equations used by M. Clynes (7), and also in the latter part of this thesis, have differences which should be corrected or explained by further experimental studies. Since neither of the equations have been rigorously derived, the initial work should be an attempt to mathematically justify or repudiate the use of these equations; then proceed with the appropriate experimental verifications.

Another obvious need is for the determination of the brain transfer functions from the carotid sinus nerve to the vagus nerve. In this report the transfer function was postulated to be a constant and time delay, but no experimental verification was attempted.

This work has attempted to use and partially evaluate the state variable formulation in the study of body control systems. The conclusions drawn are based on the theoretical development of a single body control system. This system has many elements within its control loop which are representative of other systems in the body; therefore, it is hoped that the conclusions drawn may be useful in deciding whether state variable analysis is the method to use in future problems. The disadvantages pointed out are the need for a digital computer and the difficulty in adjusting variables during simulation studies of particular systems. The advantages are ease in incorporating input signal dependent transfer functions, exact formulation for stepwise changing parameters, and advantages in analyzing nonlinear problems.

IX. LITERATURE CITED

1. Amory, D. W. and West, T. C. Chronotropic response following direct electrical stimulation of the isolated sinoatrial node: a pharmacologic evaluation. *Journal of Pharmacology and Experimental Therapeutics* 137: 14-23. 1962.
2. Bronk, D. W. and Ferguson, L. K. Impulses in cardiac sympathetic nerves. *Society for Experimental Biology and Medicine Proceedings* 30: 339-341. 1932.
3. Bronk, D. W. and Stella, G. The response to steady pressures of single end organs in the isolated carotid sinus. *American Journal of Physiology* 110: 708-714. 1935.
4. Brown, B. V. and Hilton, J. G. Baroreceptor reflexes in dogs under chloralose anesthesia. *American Journal of Physiology* 183: 433-437. 1955.
5. Cantarow, A. and Schepartz, B. *Biochemistry*. 3rd ed. Philadelphia, Pa., W. B. Saunders Co. c1962.
6. Chungcharoen, M., De Burgh Daly, N. E. and Schweitzer, A. The effect of carotid occlusion upon the intra sinus pressure with special reference to vascular communications between carotid and vertebral circulations in the dog, cat and rabbit. *Journal of Physiology* 117: 56-76. 1952.
7. Clynes, M. Respiratory sinus arrhythmia: laws derived from computer simulation. *Journal of Applied Physiology* 15: 863-874. 1960.
8. Clynes, M. Unidirectional rate sensitivity: a biocybernetic law of reflex and humoral systems as physiologic channels of control and communication. *New York Academy of Sciences Annals* 92: 946-969. 1961.
9. Downman, C. B. B. Cerebral destination of splanchnic afferent impulses. *Journal of Physiology* 113: 431-441. 1951.
10. Fruton, J. S. and Simmonds, S. *General biochemistry*. 2nd ed. New York, N.Y., John Wiley and Sons, Inc. c1958.
11. Gibson, J. E. and Pearson, J. B. The state variable formulation in problems of automatic control. Unpublished paper presented at the National Electronics Conference, Chicago, Ill., October 1963. Mimeo. Lafayette, Ind., School of Electrical Engineering, Purdue University. Ca. 1963.
12. Gould, S. E. *Pathology of the heart*. Springfield, Ill., Charles C. Thomas, c1960.

13. Grodins, F. S. Control theory and biological control systems. New York, N.Y., Columbia University Press. c1963.
14. Hahn, W. Theory and application of Liapunov's direct method. Englewood Cliffs, N.J., Prentice-Hall, Inc., c1960.
15. Heymanns, C. and Bouckaert, J. J. On the reflex regulation of the cerebral blood flow and the cerebral vaso-motor tone. *Journal of Physiology* 84: 367-380. 1935.
16. Heymanns, C. and Bouckaert, J. J. Sinus caroticus and respiratory reflexes. *Journal of Physiology* 69: 254-266. 1930.
17. Hufnagel, R. E. Analysis of aperiodically sampled-data feedback control systems. [Microfilm copy, unpublished Ph.D. thesis, Cornell University, Ithaca, N.Y.]. Ann Arbor, Mich., University Microfilms. 1959.
18. Jones, R. W., Li, C. C., Meyer, A. U. and Pinter, R. B. Pulse modulation in physiological systems, phenomenological aspects. *Institute of Electrical and Electronics Engineers, Transactions on Bio-Medical Electronics, BME-8, No. 1: 59-67. 1961.*
19. Jury, E. I. and Pavlidis, T. A literature survey of biocontrol systems. *Institute of Electrical and Electronics Engineers, Transaction on Automatic Control, AC-8, No. 3: 210-217. 1963.*
20. Kalman, R. E. and Bertram, J. E. A unified approach to the theory of sampling systems. *Franklin Institute Journal* 267: 405-436. 1959.
21. Krasovskii, N. N. Theorems on stability of motions determined by a system of two equations. (translated title) *Prikladnaja Matematika i Mekhanika* 16: 547-554. 1952. Original available but not translated; summarized in Hahn, W. Theory and application of Liapunov's direct method. p. 45. Englewood Cliffs, N.J., Prentice-Hall, Inc., c1960.
22. La Salle, J. and Lefschetz, S. Stability by Liapunov's direct method. New York, N.Y., Academic Press, Inc. c1961.
23. Liapunov, A. M. Probleme general de la stabilite du mouvement. *Annals of Mathematical Studies, No. 17. 1947.*
24. Miller, M. E. Guide to the dissection of the dog. Ann Arbor, Mich., Edwards Brothers, Inc. c1952.
- 25. Paintal, A. S. A study of right and left atrial receptors. *Journal of Physiology* 120: 596-610. 1953.
26. Ranson, S. W. and Clark, S. L. The anatomy of the nervous system. 10th ed. Philadelphia, Pa., W. B. Saunders Co. c1959.

27. Rashevsky, N. Mathematical biophysics. Volumes 1 and 2. 3rd ed. New York, N.Y., Dover Publishing, Inc. 1960.
28. Ross, A. E. Theoretical study of pulse-frequency modulation. Institute of Electrical and Electronics Engineers Proceedings 37: 1277-1286. 1949.
29. Routh, E. J. Advanced dynamics of a system of rigid bodies. 6th ed. London, Eng., Macmillan Co. 1905.
30. Ruch, T. C. and Fulton, J. E. Medical physiology and biophysics. 18th ed. Philadelphia, Pa., W. B. Saunders Co. c1960.
31. Schmidt, C. F. Carotid sinus reflexes to the respiratory center. I. American Journal of Physiology 102: 95-118. 1932.
32. Schmidt, C. F. Carotid sinus reflexes to the respiratory center. II. American Journal of Physiology 102: 119-137. 1932.
33. Scott, J. C. and Reed, E. A. Electrocardiographic effects on reflex vagal stimulation. American Journal of Physiology 167: 441-449. 1951.
34. Thaler, G. J. and Pastel, M. P. Analysis and design of nonlinear feedback control systems. New York, N.Y., McGraw-Hill Book Co., Inc. c1962.
35. Urnas, B. Central cardiovascular control. In Field, J., Magoin, H. W., and Hall, V. E., eds. Handbook of Physiology. Volume 1. Neurophysiology. Washington, D.C., American Physiological Society. 1959.
36. Wang, S. C. and Borison, H. L. Analysis of the carotid sinus cardiovascular reflex mechanism. American Journal of Physiology 150: 712-728. 1947.
37. Warner, H. R. The use of an analog computer for analysis of control mechanisms in the circulation. Institute of Electrical and Electronics Engineers Proceedings 47: 1913-1916. 1959.
38. Warner, H. R. and Cox, A. A mathematical model of heart rate control by sympathetic and vagus efferent information. Journal of Applied Physiology 17: 349-355. 1962.
39. Witt, D. B., Katz, L. W. and Kahn, L. Respiratory failure following denervation of the carotid sinus regions. American Journal of Physiology 107: 213-219. 1934.
40. Zadeh, L. A. and Desoer, C. A. Linear system theory. New York, N.Y., McGraw-Hill Book Co., Inc. c1963.

X. ACKNOWLEDGEMENTS

The author wishes to express his appreciation for the guidance offered by his major professor, Dr. H. W. Hale. The author is indebted to Dr. N. R. Cholvin for his suggestions and invaluable surgical work during the preparation of the experimental animals. Also, the laboratory assistance and suggestions of Allen Metz and Randy Mertens, undergraduate students in the College of Veterinary Medicine, are certainly appreciated.

This investigation was supported by a Public Health Service fellowship 1-F1-GM-21, 481-01A1 from the National Institute of General Medical Sciences, this welcome and appreciated support enabled the author to work full time toward the completion of this project.

XI. APPENDIX A

A. Formulation of Matrix Equations for Transfer From $R(t)$ to $V(t)$

Manfred Clynes' (7) analog representation of the respiratory sinus arrhythmia mechanism is especially suited to illustrate, first, the method of finding the transition matrix $\phi(\Delta t)$ discussed in Chapter II and, second, the case of incorporating a decision process by which different transfer functions may be used during simulation of a specific system. As has been mentioned before, this development assumes the availability of a digital computer for the matrix manipulations and decision labor.

The system representation for respiration effects on heart rate proposed by Clynes can be drawn schematically as in Figure 23. Clynes used thorax circumference, R , as a measure of respiration and two transfer functions, one during inspiration, $\frac{dR}{dt} > 0$, and one during expiration, $\frac{dR}{dt} < 0$. The output from the first block is vagal stimulation frequency, and this is used as a parameter in the nonlinear oscillator equation shown in the last block. The function $y(t)$ of the last block has the same period as the heart activity.

Since the first block of Figure 23 will be the only one influenced by the input, R , it will be considered alone and the nonlinear oscillator block, which is not affected by R , will be analyzed separately. The separation of transfer functions results in less storage space needed in a digital computer, and also a shorter program when compared to the needs of a complete program for the total system.

To begin the analysis, it can be shown that the transfer functions of Block 1 in Figure 23 correspond to the differential equations

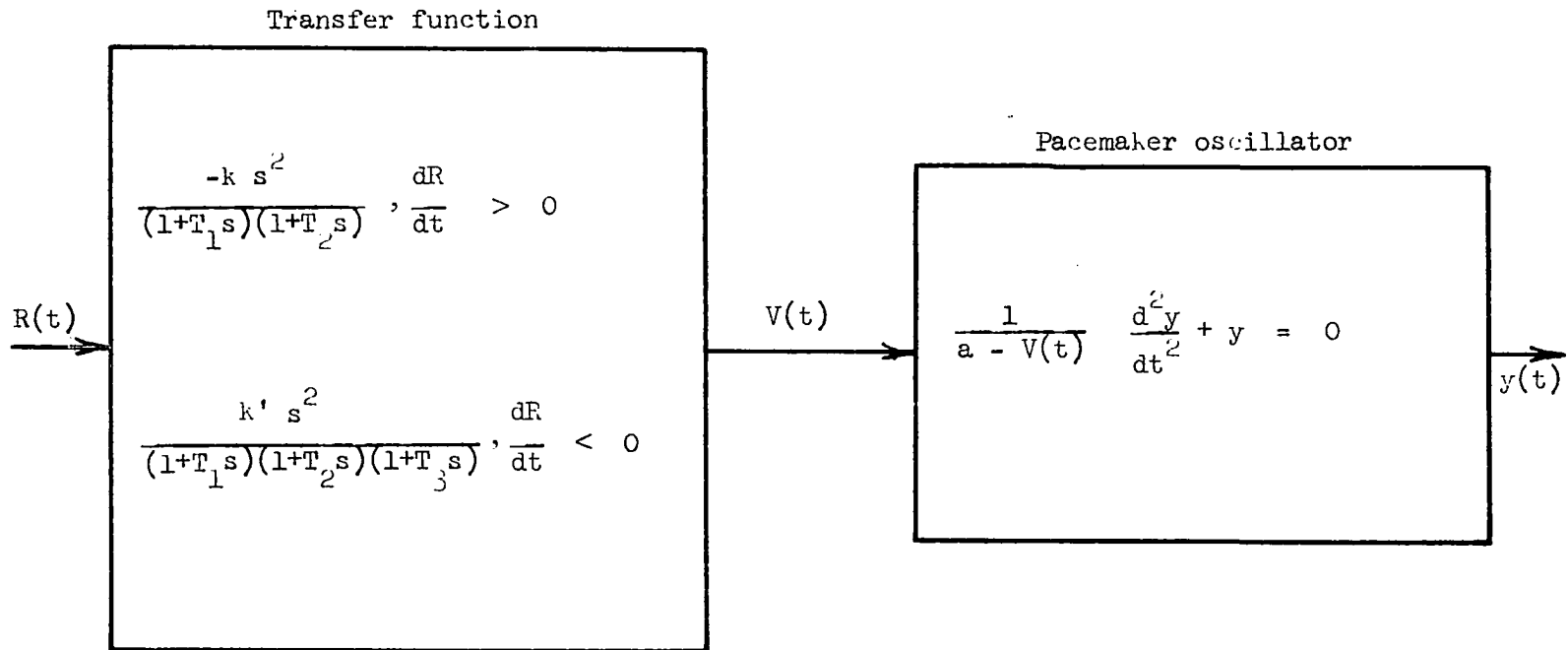


Figure 23. Schematic representation of mathematical relation between thorax circumference, $R(t)$ and heart rate (7, Clynes, Figure 13)

$$\frac{d^2V}{dt^2} + \frac{T_1+T_2}{T_1 T_2} \frac{dV}{dt} + \frac{V}{T_1 T_2} + \frac{k}{T_1 T_2} \frac{d^2R}{dt^2} = 0 \quad \frac{dR}{dt} > 0 \quad (\text{A.1})$$

and

$$\frac{d^3V}{dt^3} + \frac{T_1 T_2 + T_2 T_3 + T_3 T_1}{T_1 T_2 T_3} \frac{d^2V}{dt^2} + \frac{T_1 + T_2 + T_3}{T_1 T_2 T_3} \frac{dV}{dt} + \frac{V}{T_1 T_2 T_3} - \frac{k}{T_1 T_2 T_3} \frac{d^2R}{dt^2} = 0$$

$$\frac{dR}{dt} < 0. \quad (\text{A.2})$$

If the following substitutions are made,

$$V = x_1, \quad \frac{dV}{dt} = x_2 = \dot{x}_1, \quad \frac{d^2V}{dt^2} = x_3 = \dot{x}_2, \quad \text{and } T_a = \frac{T_1+T_2}{T_1 T_2}, \quad T_b = \frac{1}{T_1 T_2},$$

$$T_c = \frac{T_1 T_2 + T_2 T_3 + T_3 T_1}{T_1 T_2 T_3}, \quad T_d = \frac{T_1 + T_2 + T_3}{T_1 T_2 T_3}, \quad T_e = \frac{1}{T_1 T_2 T_3},$$

Equations A.1 and A.2 are then equivalent to the state variable equations

$$\dot{x}_1 = x_2 \quad (\text{A.3})$$

$$\dot{x}_2 = -T_a x_2 - T_b x_1 - k T_b \frac{d^2R}{dt^2} \quad \text{for } \frac{dR}{dt} > 0 \quad (\text{A.4})$$

and

$$\dot{x}_1 = x_2 \quad (\text{A.5})$$

$$\dot{x}_2 = x_3 \quad \text{for } \frac{dR}{dt} < 0. \quad (\text{A.6})$$

$$\dot{x}_3 = T_c x_3 - T_d x_2 - T_e x_1 + k T_e \frac{d^2R}{dt^2} \quad (\text{A.7})$$

In matrix notation, these equations will be

$$\begin{bmatrix} \dot{x}_1 \\ \dot{x}_2 \end{bmatrix} = \begin{bmatrix} 0 & 1 \\ -T_b & -T_a \end{bmatrix} \begin{bmatrix} x_1 \\ x_2 \end{bmatrix} + \begin{bmatrix} 0 \\ -kT_b \frac{d^2R}{dt^2} \end{bmatrix}, \quad \text{for } \frac{dR}{dt} > 0 \quad (\text{A.8})$$

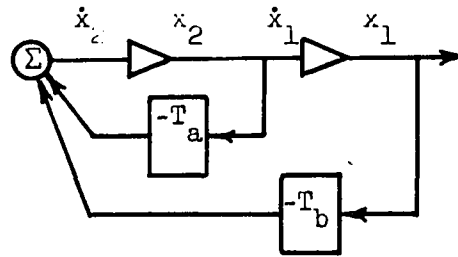
and

$$\begin{bmatrix} \dot{x}_1 \\ \dot{x}_2 \\ \dot{x}_3 \end{bmatrix} = \begin{bmatrix} 0 & 1 & 0 \\ 0 & 0 & 1 \\ -T_e & -T_d & -T_c \end{bmatrix} \begin{bmatrix} x_1 \\ x_2 \\ x_3 \end{bmatrix} + \begin{bmatrix} 0 \\ 0 \\ k'T_e \frac{d^2R}{dt^2} \end{bmatrix}, \quad \text{for } \frac{dR}{dt} < 0. \quad (\text{A.9})$$

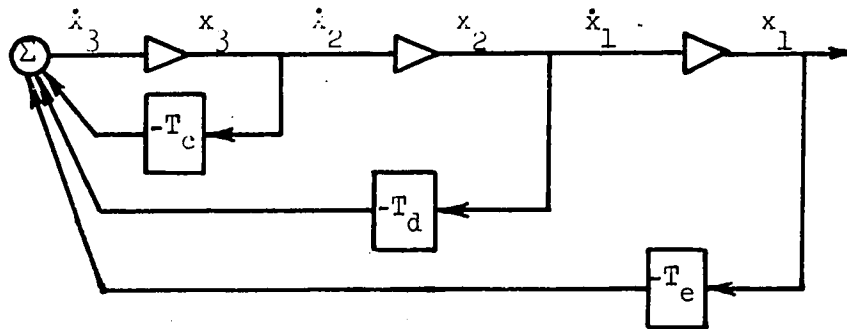
It can be verified that the analog diagrams of Figure 24a and 24b represent their respective matrix Equations A.8 and A.9 with no inputs. Using the method of direct analog computation of the $\phi(t)$ matrix of Chapter II, the result is

$$\phi(t) = \int_{\text{ins}}^{-1} \begin{bmatrix} \frac{s+T_a}{s(s+T_a)+T_b} & \frac{1}{s(s+T_a)+T_b} \\ \frac{-T_b}{s(s+T_a)+T_b} & \frac{s}{s(s+T_a)+T_b} \end{bmatrix} \quad (\text{A.10})$$

and



(a) Inspiration



(b) Expiration

Figure 24. Analog diagrams for (a) Inspiration and (b) Expiration

$$\varphi(t)_{\text{exp}} = \int_0^t e^{-\alpha t} \begin{bmatrix} \frac{s(s+T_c)+T_d}{M} & \frac{s+T_c}{M} & \frac{1}{M} \\ \frac{-T_e}{M} & \frac{s(s+T_c)}{M} & \frac{s}{M} \\ \frac{-T_e s}{M} & \frac{-(sT_d+T_c)}{M} & \frac{s^2}{M} \end{bmatrix} \quad (\text{A.11})$$

where $M = s^2(s+T_c)+T_d s+T_e$.

These results can be checked by the matrix inversion method. For the $\varphi(t)_{\text{ins}}$, corresponding to inspiration,

$$[sI-A] = \begin{bmatrix} s & -1 \\ T_b & s+T_a \end{bmatrix} \quad (\text{A.12})$$

The adjoint of this matrix is:

$$\text{Adj}[sI-A] = \begin{bmatrix} s+T_a & 1 \\ -T_b & s \end{bmatrix} \quad (\text{A.13})$$

To obtain the inverse of $[sI-A]$, its adjoint is divided by the determinant of $[sI-A]$ and

$$\underline{\phi}(t) = \int_{\text{ins}}^{-1} ([sI-A]^{-1}) = \int^{-1} \begin{bmatrix} \frac{s + T_a}{s(s+T_a)+T_b} & \frac{1}{s(s+T_a)+T_b} \\ \frac{-T_b}{s(s+T_a)+T_b} & \frac{s}{s(s+T_a)+T_b} \end{bmatrix} \quad (\text{A.14})$$

This agrees exactly with the previous equations obtained from the analog block diagram.

The form that each element of $\underline{\phi}(t)$ and $\phi(t)$ assumes is dependent on the nature of the constants T_a , T_b , T_c , etc. Since this treatment is intended only as an example of the analog diagram method of finding the $\underline{\phi}(t)$ matrix, the substitution of numerical values for these constants and the subsequent transformation from the s-domain to the time domain will not be done here.

After finding $\underline{\phi}(t)$ and $\phi(t)$, the matrix solution can be written as

$$\underline{X}(t_{n+1}) = \int_{\text{ins}}^{-1} \phi(t_{n+1}-t_n) \underline{X}(t_n) + \int_{t_n}^{t_{n+1}} \phi(t_{n+1}-\tau) \begin{bmatrix} 0 \\ -kT_b \frac{d^2 R}{dt^2} \end{bmatrix} d\tau, \quad \frac{dR}{dt} > 0, \quad (\text{A.15})$$

$$\underline{X}(t_{n+1}) = \int_{\text{exp}} \phi(t_{n+1}-t_n) \underline{X}(t_n) + \int_{t_n}^{t_{n+1}} \phi(t_{n+1}-\tau) \begin{bmatrix} 0 \\ k'T \frac{d^2 R}{dt^2} \end{bmatrix} d\tau, \quad \frac{dR}{dt} < 0. \quad (\text{A.16})$$

B. Formulation of Nonlinear Oscillator Equations

The nonlinear oscillator which Clynes used as a representation of the pacemaker potential is as follows:

$$\frac{d^2 y}{dt^2} + [a - V(t)]y = 0, \quad (\text{A.17})$$

where the period of heart rate is measured by computing the distances between successive peaks of the function $y(t)$. $V(t)$ is the vagal stimulation frequency, which corresponds to $x_1(t)$ of Equations A.8 and A.9. The constant a is

$$a = 4\pi^2 r_0^2 \quad (\text{A.18})$$

where r_0 is the normal heart rate with no vagal inhibition.

If $[a - V(t)]$ is considered constant over the iteration interval (this can be approximately realized by making the iteration time, Δt_n , small) and the following substitutions are made in Equation A.17,

$$x_2 = \dot{y}, \quad x_1 = y, \quad \dot{x}_1 = x_2,$$

the result is

$$\dot{x}_2 + (a - V(t_n)) x_1 = 0. \quad (\text{A.19})$$

The resulting state variable format is:

$$\dot{x}_1 = x_2 \quad (\text{A.20})$$

$$\dot{x}_2 = -(a - V(t_n)) x_1. \quad (\text{A.21})$$

In matrix notation,

$$\begin{bmatrix} \dot{x}_1 \\ \dot{x}_2 \end{bmatrix} = \begin{bmatrix} 0 & 1 \\ -(a-V(t_n)) & 0 \end{bmatrix} \begin{bmatrix} x_1 \\ x_2 \end{bmatrix} . \quad (\text{A.22})$$

Let,

$$A(t_n) = a-V(t_n) \quad (\text{A.23})$$

and compute

$$[sI-A] = \begin{bmatrix} s & -1 \\ A(t_n) & s \end{bmatrix} . \quad (\text{A.24})$$

The inverse, considering $A(t_n)$ constant, is

$$[sI-A]^{-1} = \begin{bmatrix} \frac{s}{s^2+A(t_n)} & \frac{1}{s^2+A(t_n)} \\ \frac{-A(t_n)}{s^2+A(t_n)} & \frac{s}{s^2+A(t_n)} \end{bmatrix} . \quad (\text{A.25})$$

From this,

$$\phi(\Delta t_n) = \begin{bmatrix} \cos A(t_n)\Delta t_n & \frac{1}{A(t_n)} \sin A(t_n)\Delta t_n \\ -\sin A(t_n)\Delta t_n & \cos A(t_n)\Delta t_n \end{bmatrix} . \quad (\text{A.26})$$

Substituting $a-V(t_n)$ back for $A(t_n)$ and writing the entire matrix equation

$$\begin{bmatrix} x_1(t_{n+1}) \\ x_2(t_{n+1}) \end{bmatrix} = \begin{bmatrix} \cos[(a-V(t_n))\Delta t_n] & \frac{1}{(a-V(t_n))} \sin[(a-V(t_n))\Delta t_n] \\ -\sin[(a-V(t_n))\Delta t_n] & \cos[(a-V(t_n))\Delta t_n] \end{bmatrix} \begin{bmatrix} x_1(t_n) \\ x_2(t_n) \end{bmatrix} \quad (\text{A.27})$$

This equation relates the variables x_1 and x_2 at t_n to their new values at t_{n+1} only if the iteration interval Δt_n is small with regard to the variation of $V(t)$. $x_2(t_n)$ corresponds to the output y , of the nonlinear oscillator in Figure 25. The digital computer can be programmed to measure the distance between maximums of the function $y(t)$. This distance can be used as the measure of period for the simulated heart rate.

Figure 26 is a schematic diagram of the computer logic needed to simulate the respiratory arrhythmia on a digital computer.

Once the function R has been converted to digital form, it is operated on by the program to obtain $\frac{dR}{dt}$. From the sign of this value the correct matrix operation is chosen and the second derivative of R is computed. The result of the matrix operations is fed into the nonlinear oscillator simulation. Here it is processed to produce an output specifying the variation in period of the heart rate.

The iteration rate is a critical consideration in the nonlinear oscillator equations because of the time varying $\phi(t)$ matrix. Since this matrix depends upon the prior solution of the inspiration and expiration

equations for the vagal stimulation frequency $V(t)$, it also places a restriction on the iteration rate of these equations. Since the variations in respiratory movements are relatively slow (16 breaths per minute), it is evident that the iteration rate need not be so slow that the computation times will be excessive.

This development gives an example of the analog method of computing the $\underline{\phi}(\Delta t_n)$ matrix. A brief description of a scheme for implementing the solution of the respiratory sinus arrhythmia reflex on a digital computer is given. From this analysis it is hoped the reader gained a better understanding of the methods as well as possible advantages and disadvantages of the proposed state variable simulation scheme.

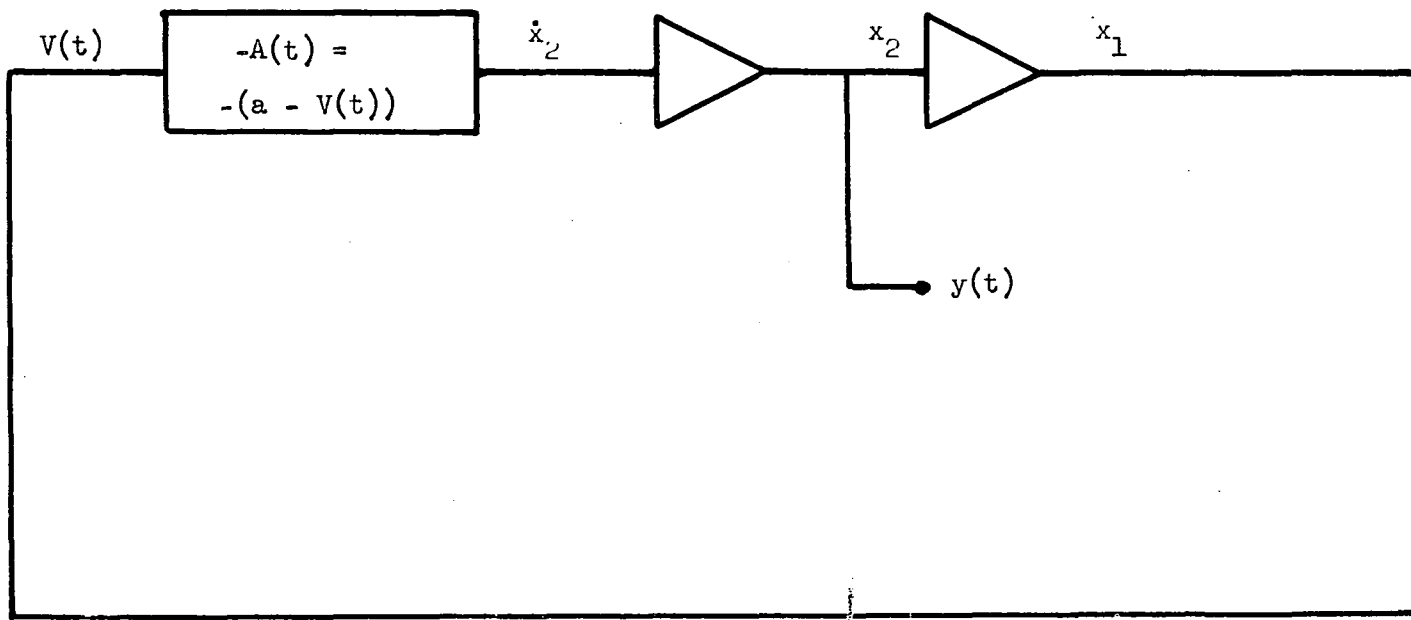


Figure 25. Analog diagram for nonlinear oscillator

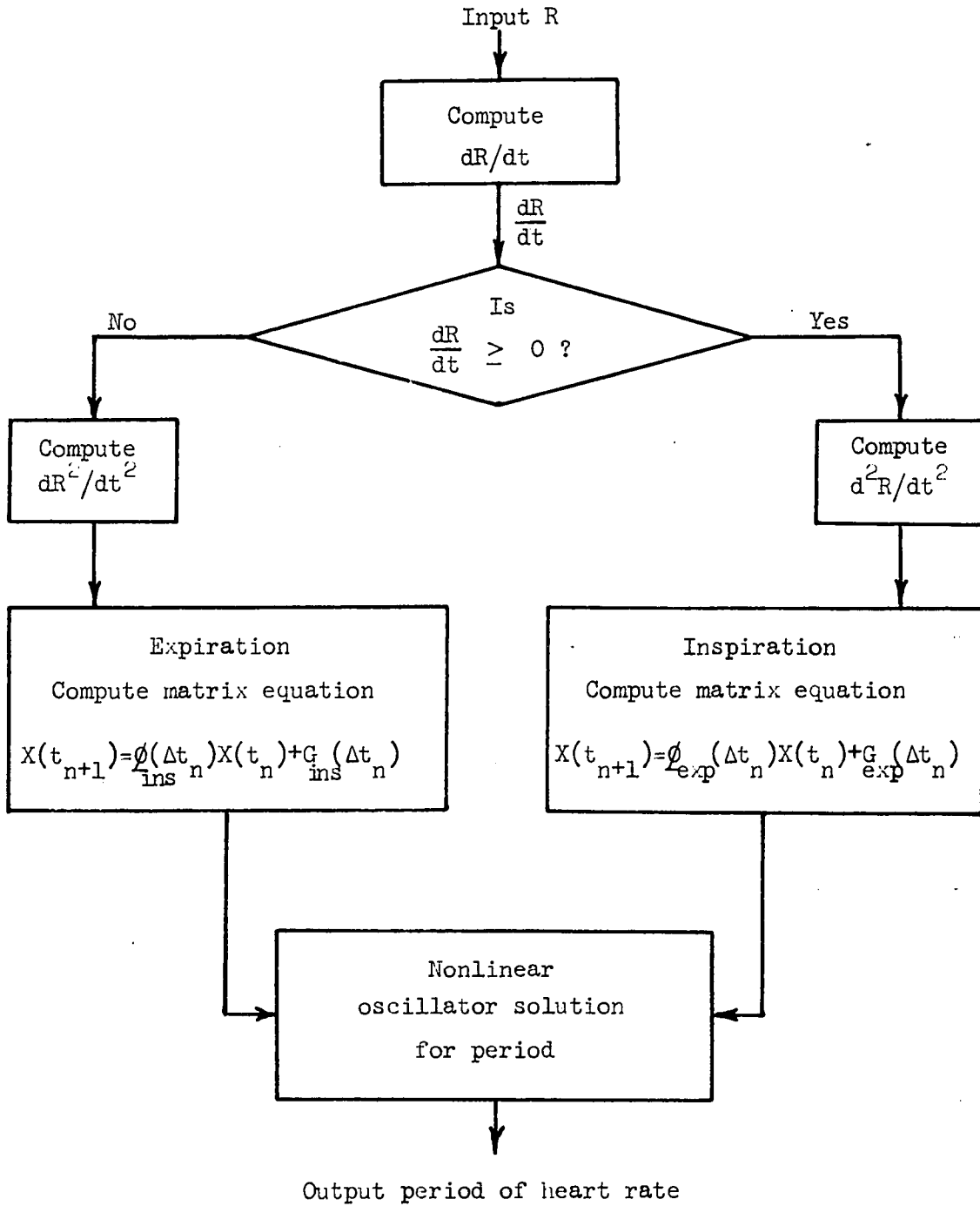


Figure 26. Schematic diagram of computer logic used to simulate respiratory sinus arrhythmia

XIII. APPENDIX B

The purpose of this appendix is to present the piecewise solution of the modified equations for the pacemaker acetylcholine concentration with $f_2(t)$ equal to a constant f_2 . These equations are discussed in Chapter III and are similar to those developed by Warner and Cox (38).

Referring to Figure 3, the equations to be solved are

$$\frac{dN(t)}{dt} = -(k_7 + k_8 f_2) N(t) + k_7 N_m \quad (\text{B.1})$$

$$\frac{dC_2(t)}{dt} = \frac{nk_8 C_1 f_2}{V_2} N(t) - \frac{k_9}{V_2} C_2(t) \quad \text{for } C_2(t) \leq C_s, \quad (\text{B.2})$$

and

$$\frac{dN(t)}{dt} = -(k_7 + k_8 f_2) N(t) + k_7 N_m \quad (\text{B.3})$$

$$\frac{dC_2(t)}{dt} = \frac{nk_8 C_1 f_2}{V_2} N(t) - \frac{k_9}{V_2} C_s \quad \text{for } C_2(t) > C_s. \quad (\text{B.4})$$

If f_2 is considered a constant and

$$A = k_7 + k_8 f_2, \quad B = k_7 N_m,$$

$$C = \frac{nk_8 f_2 C_1}{V_2}, \quad \text{and} \quad D = \frac{k_9}{V_2} C_s$$

Equations B.1 and B.2 will be

$$\frac{dN(t)}{dt} = -AN(t) + B \quad (\text{B.5})$$

$$\frac{dC_2(t)}{dt} = CN(t) - DC_2(t) . \quad (B.6)$$

Taking the Laplace transform of these equations and rearranging,

$$C_2(s) = \frac{CN(s) + C(0+)}{s + D} \quad (B.7)$$

$$N(s) = \frac{B + sN(0+)}{s(s + A)} \quad (B.8)$$

Substituting Equation B.8 into Equation B.7 for $N(s)$ and separating into partial fractions,

$$C_2(s) = CB \left[\frac{1}{ADs} + \frac{1}{(-A)(D-A)} \frac{1}{s + A} + \frac{1}{(-D)(A-D)} \frac{1}{s + D} \right] \\ + CN(0+) \left[\frac{1}{D-A} \frac{1}{s + A} + \frac{1}{A - D} \frac{1}{s + D} \right] + \frac{C(0+)}{s + D} . \quad (B.9)$$

To find $C_2(\infty)$, a well known property of Laplace transform theory,

$$\lim_{t \rightarrow \infty} C_2(t) = \lim_{s \rightarrow 0} sC_2(s), \quad (B.10)$$

is used. Applying Equation B.10 to Equation B.9 and substituting for A, B, C, and D gives

$$\lim_{t \rightarrow \infty} C_2(t) = \frac{CB}{AD} = \frac{nk_8 C_1 N f_2}{k_9 \left(1 + \frac{k_8 f_2}{k_7} \right)} . \quad (B.11)$$

This equation agrees in form to that obtained by Warner and Cox (35) for

$$C_2(\infty) \text{ when } C_2(t) \leq C_s .$$

When $C_2(t) > C_s$, letting A, B, and C equal the previous values and

$$E = \frac{k_9}{V_2} C_s, \quad (\text{B.12})$$

Equations B.3 and B.4 become

$$\frac{dN(t)}{dt} = -AN(t) + B \quad (\text{B.13})$$

and

$$\frac{dC_2(t)}{dt} = CN(t) - E. \quad (\text{B.14})$$

Then taking the Laplace transform of Equation B.14 and substituting Equation B.8 for $N(s)$,

$$C_2(s) = \frac{C_2(0^+)}{s} + \frac{CN(0^+)}{s(s+A)} + \frac{CB}{s^2(s+A)} - \frac{E}{s^2}. \quad (\text{B.15})$$

Taking the inverse Laplace transform,

$$C_2(t) = C_2(0^+) + \frac{CN(0^+)}{A} (1 - e^{-At}) + \frac{CB}{A^2} e^{-At} - \frac{CB}{A^2} + \left(\frac{CB}{A} - E\right)t. \quad (\text{B.16})$$

Then the

$$\lim_{t \rightarrow \infty} C_2(t) = C_2(0^+) + \frac{CN(0^+)}{A} - \frac{CB}{A^2} + \lim_{t \rightarrow \infty} \left(\frac{CB}{A} - E\right)t. \quad (\text{B.17})$$

If the initial values for $C_2(0^+)$ and $N(0^+)$ are assumed to be

$$C_2(0^+) = C_s$$

$N(0^+) = [\text{Any value from zero to } N_m \text{ is possible, but, use } N_m \text{ for computations}]$

Then

$$\begin{aligned} \lim_{t \rightarrow \infty} C_2(t) &= C_s + \frac{C N_m}{A} - \frac{C k_7 N_m}{A^2} + \lim_{t \rightarrow \infty} \left(\frac{CB}{A} - E \right) t \\ &= C_s + \frac{C N_m}{A} \left(1 - \frac{k_7}{A} \right) + \lim_{t \rightarrow \infty} \left(\frac{CB}{A} - E \right) t . \end{aligned} \quad (\text{B.18})$$

Since

$$C_s + \frac{C N_m}{A} \left(1 - \frac{k_7}{A} \right) \geq 0, \quad (\text{B.19})$$

because

$$1 - \frac{k_7}{A} = 1 - \frac{k_7}{k_7 + k_8 f_2} \geq 0, \quad (\text{B.20})$$

it is evident that

$$\lim_{t \rightarrow \infty} C_2(t) = +\infty \quad (\text{B.21})$$

if

$$\frac{CB}{A} > E . \quad (\text{B.22})$$

From Equation B.16, if $\frac{CB}{A} = E$, it is evident $C_2(t)$ does not approach infinity as time becomes large. But if

$$\frac{CB}{A} < E, \quad (\text{B.23})$$

as time increases the last term of Equation B.18 will eventually cancel out the second term at some time, t_c , and leave only

$$C_2(t_c) = C_s. \quad (\text{B.24})$$

At that point the mathematical description must be changed to the previous equations for $C_2(t) \leq C_s$ and they have been shown to be stable. Thus, the inequality

$$\frac{CB}{A} \leq E$$

must be satisfied for stability of the concentration of acetylcholine, $C_2(t)$. Substituting for A, B, C, and E and rearranging, for stability,

$$f_2 \leq \frac{C_s}{\frac{nk_8 C_1 N}{k_9} - \frac{k_8 C_s}{k_7}}.$$

This is the same inequality as that obtained by Liapunov's Second Method in Chapter III except for the equality sign.

XIII. APPENDIX C

A. Description of Method

The problem is to compute a curve describing the period of heart rate when given the following conditions.

1. The input signal or disturbance is a step function of pressure on the carotid sinus of magnitude equal to 300 mm. Hg. This can be mathematically written as

$$P(t) = 300 u(t) \quad (C.1)$$

where $u(t)$ represents a unit step from $t = 0$ to $t = \infty$.

2. The relationship between carotid sinus impulse frequency and perfusion pressure $P(t)$ is

$$\tau \frac{df_1(t)}{dt} + f_1(t) = k_1 \frac{d(P(t)-50)}{dt} + k_2(P(t)-50) \quad (C.2)$$

3. The effect of the brain is represented by the relation

$$f_2(t) = K_b f_1(t - \tau_b). \quad (C.3)$$

4. The pacemaker acetylcholine concentration is described by the following matrix equation from Chapter V.

$$\begin{bmatrix} N(t_{n+1}) \\ C_2(t_{n+1}) \end{bmatrix} = \begin{bmatrix} e^{-(2.75+0.69f_2)\Delta t_n} & 0 \\ \frac{0.565f_2[e^{-0.87\Delta t_n} - e^{-(2.75+0.69f_2)\Delta t_n}]}{N_m k_{10}(1.88 + 0.69f_2)} & e^{-0.87\Delta t_n} \end{bmatrix} \begin{bmatrix} N(t_n) \\ C_2(t_n) \end{bmatrix}$$

$$+ \left[\frac{2.75N_m}{2.75+0.69f_2} [1-e^{-(k_7+k_8f_2)\Delta t_n}] \right. \\ \left. \frac{1.55 f_2}{k_{10}(1.88+0.69f_2)} \left(\frac{1}{0.87} (1-e^{-0.87\Delta t_n}) - \frac{(1-e^{-(2.75+0.69f_2)\Delta t_n})}{2.75+0.69f_2} \right) \right] \quad (C.4)$$

The method of obtaining the frequency $f_2(t)$ for the matrix equations is described below and the analysis is influenced by results and discussions in Grodins (13), and Jones, et al. (18).

The differential equation used to describe the relation between carotid sinus impulse frequency and carotid sinus perfusion pressure is

$$\tau \frac{df_1(t)}{dt} + f_1(t) = k_1 \frac{dP'(t)}{dt} + k_2 P'(t) \quad (C.5)$$

where

$$P'(t) = P(t) - 50 \text{ mm. Hg.} \quad (C.6)$$

Taking the Laplace transform of both sides of Equation C.5, and assuming all initial values equal to zero,

$$\tau s f_1(s) + f_1(s) = k_1 s P'(s) + k_2 P'(s). \quad (C.7)$$

Rearranging,

$$\frac{f_1(s)}{P'(s)} = \frac{k_2}{\tau s + 1} + \frac{k_1 s}{\tau s + 1} \quad (C.8)$$

If

$$P(t) = K u(t) \quad (C.9)$$

then

$$P'(s) = \frac{K}{s} - \frac{50}{s} = \frac{K-50}{s} = \frac{K'}{s} . \quad (C.10)$$

Substituting for $P'(s)$ in Equation C.8, solving for $f_1(s)$, and taking the inverse Laplace transform gives,

$$f_1(t) = K' \left[k_2 (1 - e^{-\frac{t}{\tau}}) + \frac{k_1}{\tau} e^{-\frac{t}{\tau}} \right] \quad (C.11)$$

The numerical values used to calculate $f_1(t)$ for a specified input step magnitude of pressure are determined both experimentally and by trial and error in an effort to obtain the best mathematical model of the heart rate response to a step input of pressure at the carotid sinus nodes.

The value of K' is determined by the magnitude of the step input of pressure which is

$$K = 300 \text{ mm. Hg.}$$

This determines

$$K' = (300-50) = 250 \text{ mm. Hg.}$$

The trial and error calculations for k_1 , k_2 , and τ led to the following values for a reasonable agreement between experimental and theoretical heart period response curves,

$$k_1 = \frac{11}{12} \frac{\text{pulses}}{\text{mm. Hg second}},$$

$$k_2 = \frac{1}{6} \frac{\text{pulses}}{\text{mm. Hg}},$$

and

$$\tau = \frac{2}{3} \text{ second.}$$

The action of the brain on $f_1(t)$ to produce $f_2(t)$, the vagal pulse frequency, is represented by

$$f_2(t) = K_b f_1(t - \tau_b) \quad (\text{C.12})$$

where K_b is estimated to be

$$K_b = \frac{1}{250} \frac{\text{vagal impulse}}{\text{carotid sinus nerve pulse}}.$$

The value for τ_b , obtained from the experimental evidence discussed and presented in Chapter V, is

$$\tau_b = 1 \text{ second.}$$

The entire expression for $f_2(t)$, assuming a step input of pressure and using the above constants, is

$$\begin{aligned} f_2(t) &= \frac{1}{250} f_1(t - 1) \\ &= \frac{1}{6} (1 - e^{-(t-1)}) + \frac{11}{12} \frac{3}{2} e^{-(t-1)}. \end{aligned} \quad (\text{C.13})$$

This function is plotted in Figure 27 for a step input applied at $t = 0$. The function is not piecewise constant over the entire time interval of interest and, in order to apply the transition relations of Equation C.4, $f_2(t)$ must be piecewise constant. In order to develop this type of function, an averaging scheme is employed wherein the initial transient is averaged over the significant portion of the transient and this average value used in the iteration procedures during that time interval. For the remaining portion of the record, the final value of $f_2(t)$ $_{t=\infty}$ is used.

The averaging manipulations for the transient period begin with the previous Equation C.13. Since the transient period, from observation of Figure 27, is from $t = 1$ to $t = 3$, the averaging integral will be

$$f_{2\text{ave}}(t) = \frac{1}{2} \int_1^3 \left[\frac{1}{6} (1 - e^{-(t-1)}) + \frac{11}{12} e^{-(t-1)} \right] dt. \quad (\text{C.14})$$

This integration produces the following approximate value for $f_2(t)$,

$$f_{2\text{ave}}(t) = \frac{1}{2} \quad \text{for} \quad 1 \leq 3. \quad (\text{C.15})$$

The value for t greater than three seconds is $\frac{1}{6}$ cycles per second which is obtained by using the value of $f_2(t)$ $_{t=\infty}$. The complete piecewise constant $f_2(t)$ function is the dotted curve shown in Figure 27. This process of averaging can be justified by considering the prolonged effect on the system of an impinging pulse. The effect of the pulse is not instantaneous but remains a finite time after the pulse has arrived, affecting both the amount of acetylcholine available and the amount being used. Since for high frequencies the amount of acetylcholine available is

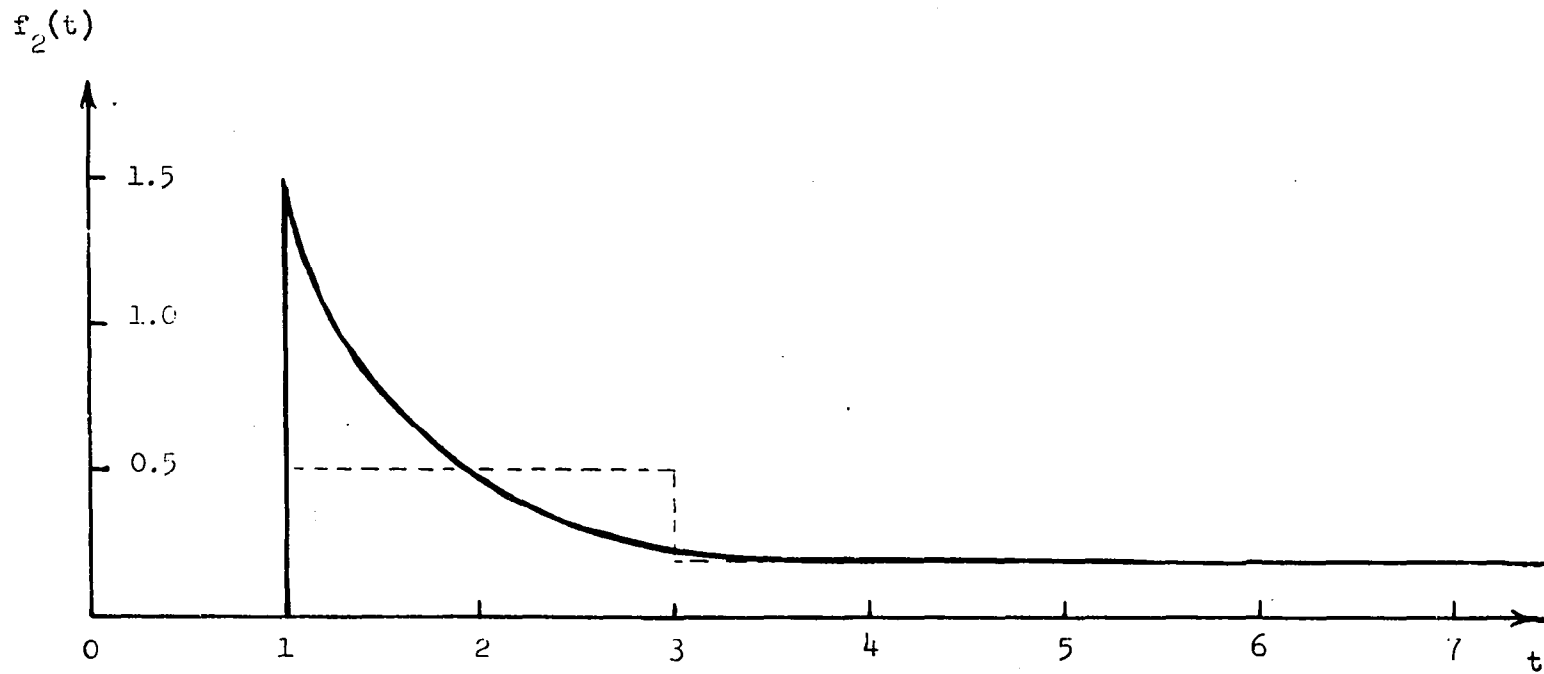


Figure 27. Vagal pulse frequency response to a step input of pressure at the carotid sinus nodes at time $t = 0$

diminished and less is excreted into the sinoatrial volume for each pulse and at low frequencies more is available, allowing more acetylcholine release per pulse, this compensatory mechanism, in effect, averages the pulse frequency during transient periods in much the same manner as is done in Figure 27.

For this specific problem, the following procedure is used (assuming initial conditions $N(0) = N_m$, $C_2(0) = 0$, and $f_2(0) = 0$) to find the heart rate period.

1. Find f_2 within the iteration interval, Δt_n , from Figure 27.
2. Calculate the elements of matrix Equation C.4.
3. Find $N(t_{n+1})$ and $C_2(t_{n+1})$, using the previous or initial values for $N(t_n)$ and $C_2(t_n)$.
4. Using the value obtained for $C_2(t)$, calculate $p(t_{n+1})$ using,

$$p(t_{n+1}) = 0.5 + k_{10} C_2(t_{n+1})$$

This procedure will be illustrated in the next section.

B. Calculations

The following is an abbreviated sample calculation for the curve shown in Figure 13 of Chapter V. The step input of Equation C.1 is impressed on the carotid sinus at $t = 0$.

1. For $0 \leq t < 1$

Because the vagal discharge is close to zero, if not zero, for zero input to the carotid sinus, it is assumed that

$$N(0) = N_m$$

$$c_2(0) = 0$$

Because of the lag of 1 second, $f(\Delta t_{0-1}) = 0$. Therefore

$$p(0) = 0.5 + k_{10}(0) = 0.5 \text{ seconds.}$$

and, also,

$$p(1) = 0.5 + k_{10}(0) = 0.5 \text{ seconds.}$$

2. For $1 \leq t < 2$

$$f(\Delta t_{1-2}) = \frac{1}{2}$$

Then,

$$\begin{bmatrix} N(2) \\ c_2(2) \end{bmatrix} = \begin{bmatrix} 0.045 \\ \frac{0.0475}{N_m k_{10}} \end{bmatrix} + \begin{bmatrix} 0 \\ 0.42 \end{bmatrix} \begin{bmatrix} N_m \\ 0 \end{bmatrix} + \begin{bmatrix} 0.85N_m \\ \frac{0.122}{k_{10}} \end{bmatrix},$$

$$N(2) = 0.895 N_m,$$

$$c_2(2) = \frac{0.170}{k_{10}}$$

and

$$p(2) = 0.5 + 0.170 = 0.670 \text{ seconds.}$$

3. For $2 \leq t < 3$

$$f(\Delta t_{2-3}) = \frac{1}{2}$$

Then,

$$\begin{bmatrix} N(3) \\ C_2(3) \end{bmatrix} = \begin{bmatrix} 0.045 \\ \frac{0.0475}{\frac{N}{m} k_{10}} \end{bmatrix} + \begin{bmatrix} 0 \\ 0.42 \end{bmatrix} \begin{bmatrix} 0.895N_m \\ \frac{0.170}{k_{10}} \end{bmatrix} + \begin{bmatrix} 0.85N_m \\ \frac{0.122}{k_{10}} \end{bmatrix},$$

$$N(3) = 0.89N_m,$$

$$C_2(3) = \frac{0.235}{k_{10}},$$

and

$$p(3) = 0.5 + 0.235 = 0.735 \text{ seconds.}$$

4. For $3 \leq t < 4$

$$f(\Delta t_{3-4}) = \frac{1}{6}$$

In this interval f_2 has changed from $\frac{1}{2}$ to $\frac{1}{6}$ and the transition equations are,

$$\begin{bmatrix} N(4) \\ C_2(4) \end{bmatrix} = \begin{bmatrix} 0.057 \\ \frac{0.0173}{\frac{N}{m} k_{10}} \end{bmatrix} + \begin{bmatrix} 0 \\ 0.42 \end{bmatrix} \begin{bmatrix} 0.89N_m \\ \frac{0.235}{k_{10}} \end{bmatrix} + \begin{bmatrix} 0.91N_m \\ \frac{0.042}{k_{10}} \end{bmatrix}.$$

Then,

$$N(4) = 0.96N_m,$$

$$C_2(4) = \frac{0.156}{k_{10}},$$

and

$$p(4) = 0.5 + 0.156 = 0.656.$$

5. For $4 \leq t < 5$

$$f(\Delta t_{4-5}) = \frac{1}{6}$$

Then,

$$\begin{bmatrix} N(5) \\ C_2(5) \end{bmatrix} = \begin{bmatrix} 0.057 \\ \frac{0.0173}{k_{10} N_m} \end{bmatrix} + \begin{bmatrix} 0 \\ 0.42 \end{bmatrix} \begin{bmatrix} 0.96 N_m \\ \frac{0.156}{k_{10}} \end{bmatrix} + \begin{bmatrix} 0.91 N_m \\ \frac{0.042}{k_{10}} \end{bmatrix},$$

$$N(5) = 0.96 N_m,$$

$$C_2(5) = \frac{0.124}{k_{10}},$$

and

$$p(5) = 0.5 + 0.124 = 0.624.$$

6. For $5 \leq t < 6$

$$f(\Delta t_{5-6}) = \frac{1}{6}$$

Then,

$$\begin{bmatrix} N(6) \\ C_2(6) \end{bmatrix} = \begin{bmatrix} 0.057 \\ \frac{0.0173}{k_{10} N_m} \end{bmatrix} + \begin{bmatrix} 0 \\ 0.42 \end{bmatrix} \begin{bmatrix} 0.96 N_m \\ \frac{0.124}{k_{10}} \end{bmatrix} + \begin{bmatrix} 0.91 N_m \\ \frac{0.042}{k_{10}} \end{bmatrix},$$

$$N(6) = 0.96 N_m,$$

$$c_2(6) = \frac{0.111}{k_{10}},$$

and

$$p(6) = 0.5 + 0.111 = 0.611 \text{ seconds.}$$

This can be continued in the same manner for succeeding points in time. The resulting curve is shown in Figure 13 of Chapter V.

Although this method and the mathematical model used, are satisfactory in the sense that they predict the experimental response fairly accurately, it would be more satisfying to know the exact response due to one pulse of stimulation at the sinoatrial node. This would entail a chemical study of the time variation of the concentration of acetylcholine at the sinoatrial node before and after a pulse has arrived. From this information a more accurate mathematical description could be attempted via the state variable formulation.